Spring 2012

Basic capillary microfluidic chip and highly sensitive optical detector for point of care application

Mingjin Yao
Louisiana Tech University

BASIC CAPILLARY MICROFLUIDIC CHIP AND

HIGHLY SENSITIVE OPTICAL DETECTOR

FOR POINT OF CARE APPLICATION

by

Mingjin Yao, B.S., M.S.

A Dissertation Presented in Partial Fulfillment
of the Requirements of the Degree
Doctor of Philosophy

COLLEGE OF ENGINEERING AND SCIENCE
LOUISIANA TECH UNIVERSITY

May 2012

UMI Number: 3515666

UMI

Dissertation Publishing

UMI 3515666

ProQuest

LOUISIANA TECH UNIVERSITY

THE GRADUATE SCHOOL
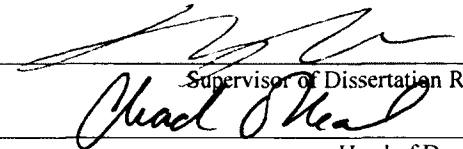
April 2, 2012

_____
Date

We hereby recommend that the dissertation prepared under our supervision

by_____Mingjin Yao_____

entitled_____

Basic Capillary Microfluidic Chip and Highly Sensitive Optical Detector
_____

for Point of Care Application
_____

_____

_____

be accepted in partial fulfillment of the requirements for the Degree of

Doctor of Philosophy in Engineering
_____

_____
Supervisor of Dissertation Research

_____
Head of Department

_____
Department

Recommendation concurred in:

_____

_____

_____
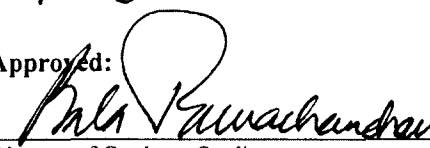
Advisory Committee

Approved:

_____
Director of Graduate Studies

_____
Dean of the College

Approved:

_____
Dean of the Graduate School

ABSTRACT

A cost-effective and highly sensitive portable diagnostic device is needed to enable much more widespread monitoring of health conditions in disease prevention, detection, and control. Miniaturized and easy-to-operate devices can reduce the inherent costs and inefficiencies associated with healthcare testing in central laboratories. Hence, clinicians are beginning to use point of care (POC) testing and flexible clinical chemistry testing devices which are beneficial for the patient.

In our work, a low-cost and simple autonomous microfluidic device for biochemical detection was developed. The pumpless capillary system with capillary stop valves and trigger valves is f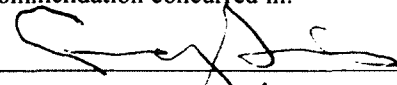abricated on a silicon (Si) wafer and then bonded with the modified polydimethylsiloxane (PDMS) cover. The key point of this study is the change of the surface contact angle of the PDMS to achieve the functionalities such as timing features (capillary-driven stop valve) and basic logical functions (trigger valves). The polydimethylsiloxane-ethylene oxide polymer (PDMS-b-PEO) is utilized as a surfactant additive to make the PDMS hydrophilic. The contact angle of the modified PDMS can be adjusted from 80.9° to 21.5° with different mixing ratios. The contact angles of PEO-PDMS accepted in this work are from 80.9° to 58.5° to bring the capillary channel and

valve into effect. This autonomous capillary-driven device with good microfluidic flow manipulation can be widely applied to a number of microfluidic devices and pumpless fluidic actuation mechanisms, which is suitable for cost-effective diagnostic tools in the biomedical analysis and POC testing applications.

Another obstacle for miniaturization of the bio-detection system is the optical detector. We developed a novel, highly sensitive and miniaturized detector. It integrates a light source--light emitting diode (LED), all necessary optical components, and a photodiode with preamplifier into one package about 2 cm × 2 cm × 2 cm, especially for the applications of lab-on-a-chip (LOC), portable bio-detection system and POC diagnostic system. The size of this detector is smaller than the existing miniaturized detector of the size 5 cm × 5 cm × 5 cm. The fluorescence dye 5-Carboxyfluorescein (5-FAM) dissolved into the solvent DMSO (Dimethyl Sulfoxide) and diluted with DI water was used as the testing solution samples. The prototype has been tested to prove a remarkable sensitivity at pico-scale molar, around 1.08 pM, which is the highest sensitivity by now. It is higher than the current limit of detection at 1.96 nm, which will be presented in detail in the latter section.

APPROVAL FOR SCHOLARLY DISSEMINATION

The author grants to the Prescott Memorial Library of Louisiana Tech University the right to reproduce, by appropriate methods, upon request, any or all portions of this Dissertation. It is understood that "proper request" consists of the agreement, on the part of the requesting party, that said reproduction is for his personal use and that subsequent reproduction will not occur without written approval of the author of this Dissertation. Further, any portions of the Dissertation used in books, papers, and other works must be appropriately referenced to this Dissertation.

Finally, the author of this Dissertation reserves the right to publish freely, in the literature, at any time, any or all portions of this Dissertation.

Author _____ Mingjin Yao _____

Date _____ 5/8/2012 _____

TABLE OF CONTENTS

LIST OF TABLES

LIST OF FIGURES

ACKNOWLEDGMENTS

I would like to thank my research and dissertation advisors, Dr. Long Que and Mr. Ji Fang, for their invaluable advice, continuous guidance, encouragement, and support throughout these years at Louisiana Tech University. They not only taught me scientific working styles and research skills, but also strict and meticulous scholarship. I would like to extend my most sincere thanks to the members of my advisory committee for this dissertation.

I would also like to thank all the faculty and staff at the Institute for Micromanufacturing for their zealous help and support on the simulation modeling, microfabrication processes as well as metrology instruments. Much gratitude is extended to Dr. Girish Shah and others of the University of Louisiana at Monroe for their helpful discussion, support and cooperation. I also give thanks to all my friends for their wonderful help during my time at Louisiana Tech University.

I thank again my advisors for their everlasting and unconditional support. Also, this dissertation is a present for my family. I thank my parents for their long-standing love and education.

CHAPTER 1

INTRODUCTION

1.1   Motivation

With the development of diagnostic technologies for the use at the POC, researchers are improving the lives of people in the world. POC takes center stage in the treatment and surveillance of infectious diseases in medicine. Also, it utilizes the latest advances in the fields of biotechnology, LOC, and miniaturization technology. In addition, the miniaturization provides the means to produce the small, fast and easy-to-operate devices for reduced-cost healthcare testing at the point of care or even for household use. These microfluidic devices have been long recommended to revolutionize the POC diagnostics. POC testing, which reduces the complications and the hospital stay space and time, is beneficial to the diagnostic or treatment strategy, and even the overall health outcome. Although POC laboratory testing is sometimes a little expensive, it produces wider economic benefits [1].

Lack of health has an incredible impact on the quality of life. Hence, disease prevention and treatment is important, which is often based on the measurement of chemical parameters in biological samples, such as blood and urine. In most cases, the samples need to be sent to a central laboratory for analysis, and the results of routine tests become available after several hours, sometimes days. Apart from the time delay and

mistakes in the logistics, such as lost samples and mislabeling, timely diagnosis may be constrained. Among the existing disease diagnosis, the POC testing enables more widespread monitoring of health parameters in disease prevention. An evolution in POC technology, indicated by an increasing number of commercially available POC testing devices, spurs a new trend for further miniaturization, the introduction of LOC devices.

The exponential growth in the current market of POC testing apparatus can be forecasted [1-2]. We believe that microchip-based analysis systems will cause a revolution in the medical area in the future. The critical medicine parameters will be monitored in the operation rooms and intensive care units of hospitals. Household analyzers and miniaturized personal laboratories will report on our daily health status. Medical decisions will be based on measurement results, immediately available at the general practitioner's office. Just like with personal computers and cellular phones, LOC devices will form an integral part of our lives sometime in the future.

Two broad types of technology that support the POC testing contain small bench top analysers (for example, blood gas and electrolyte systems) and hand held devices (such as urine albumin, blood glucose, and coagulation tests) [3-4]. The bench top systems are smaller versions of laboratory analyzers in which vulnerable operator dependent steps have been automated: for example, automatic flushing of the sample after analysis, calibration, and quality control. Hand held devices have been developed using microfabrication techniques. They are outwardly simple but internally complex devices that do several tasks, for example, separate cells from plasma, add reagents, and the red color or other end points [5].

It is almost axiomatic that providing a more rapid result saves time and therefore money. However, there will be no saving unless the result is acknowledged and action is taken. The economic benefit of POC testing can be judged in terms of the short term gain from more effective use of resources in the immediate episode of care (box). For example, use of the POC testing to assess coagulation status and platelet function has been shown to reduce the requirement for blood products. It is estimated that the POC testing could save over $250,000 a year in a research institution [1].

The biosensor and disease detection system are developing rapidly, and are also very significant at present. For example, it is reported that the most commonly diagnosed cancer accounted for 30 percent of all cancers in men is prostate cancer. In 2008, approximately 186,320 men in the United States will be diagnosed with prostate cancer and an estimated 28,660 will die from the disease [6]. Prostate cancer is second only to lung cancer as a leading cause of cancer deaths in men (reported by American Cancer Society, 2008) [7]. There have been many great efforts on the development of disease detection system and diagnosis technologies in the past decades. A host of related different immunoassay readout techniques has been developed in the past. The current established approaches include scintillation counting [2], fluorescence [3-4], chemiluminescence [5], electrochemical [6], and enzymatic methods [7]. Recently, strategies based on the surface plasmon resonance [8], surface-enhanced Raman scattering (SERS) [9], quantum dots [10], microcantilevers [11] [12], and atomic force microscopy [13] have been devised. Because of its inherently high sensitivity, fluorescence-based detection is among the most used readout modality [14]. Microbiosensors and nanobiosensors, which mainly utilize the technologies of

microelectromechanical system (MEMS) and nanoelectromechanical system (NEMS) based on nanomechanics, are of great interest to researchers and scientists in this area.

There is a challenge for the miniaturization and the quite high sensitivity of the portable detection system, which can match the POC apparatus in clinical applications. This project is motivated by the current requirements in bio-detection, biomedical, protein detection, DNA extraction, and the POC applications [15]. The existing optical POC system in the fluorescent-based detection system is either too large, or has a low sensitivity. Figure 1.1 shows a POC blood analysis unit, which tests blood gas, electrolytes and other chemistries at the POC. The POC device is designed to provide laboratory quality results, available within two minutes. An onboard thermal printer outputs results and test notes. The system functions with a capillary blood sample (there is a special collection device) as well as arterial or venous samples. It is a self-contained piece of equipment that can be easily transported between settings. This will be better for the medical application if there is a miniaturized and easy-to-use device to match the POC testing.
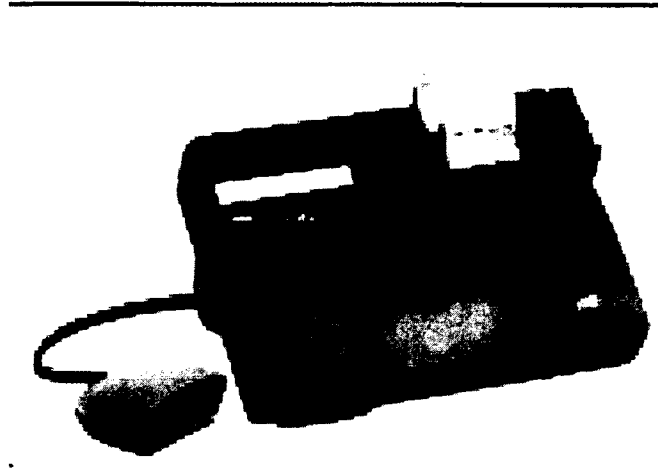
Figure 1.1 One kind of point-of-care blood analysis unit instrument [1].

Therefore, to achieve low-cost, high sensitivity, and miniaturization, it is necessary to develop a highly efficient, fluorescent-based sample detection scheme, which will enhance the sensitivity of the detector and design an autonomous microfluidic chip for flow manipulation of the sample solution with only capillary action. Some current microfluidic chips are complicated to operate, such as shown in Figure 1.2. These microfluidic chips are with a few external pumps or other actuators. Such an instrument is not simple and suitable for the portable detection system in clinical chemistry or the medical areas.
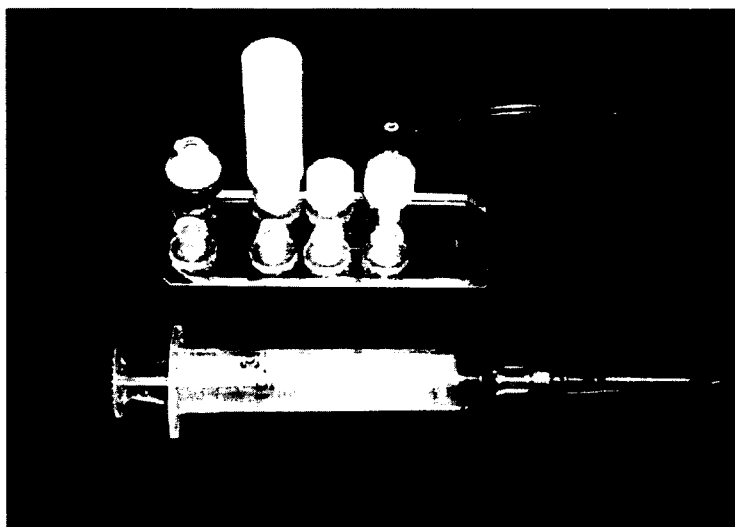
Figure 1.2 The fluid flows in a microfluidic chip by a syringe pumping [1].

1.2   Previous Research Work

There is some research done for the bio-detection system in biomedical and clinical areas due to the rapid development of the emerging microfluidics and microfabrication technologies with much more widespread monitoring of health parameters in disease prevention and biomarker monitoring in the POC diagnosis.

There have been many efforts to detect this kind of cancer and other diseases in POC applications. Current innovations in miniaturized systems have continued to rely on macroscale, external optical read-out arrangements so that they minimize the benefits of microfabrication. Currently, the detection label is usually fluorescence dye due to the high sensitivity and efficiency of the fluorescence property. Thus, fluorescence spectroscope is commonly used in medical testing or research. A fluorescence microscope, which is shown in Figure 1.3, is much the same as a conventional light microscope with added features to enhance its capabilities. A fluorescence microscope uses a much higher intensity light source, which excites a fluorescent species in a sample

of interest. This fluorescent species emits a lower energy light of a longer wavelength that produces the magnified image instead of the original light source.
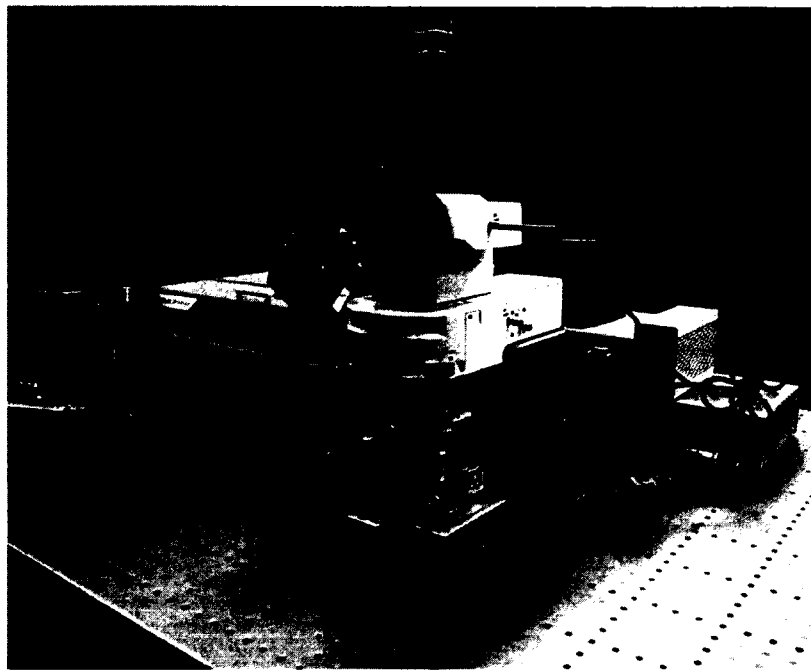
Figure 1.3 An upright fluorescence microscope with the fluorescent filter cube turret above the objective lenses, coupled with a digital camera and connecting a fluorescence spectroscopy beside template for inserting figures.

The fluorescence microscope is a powerful, yet economical, laboratory tool with a broad range of applications. They are often used in medicine, public health, biological research, and environment monitoring. The most common application is medical laboratory diagnosis due to its sensitivity, specificity, and rapid testing [16-17]. However, it is complicated to operate and has a large size as shown in Figure 1.3; therefore, it is not suitable to the micro-scale sample testing or portable testing system for POC. For some specific cases, it does not satisfy the requirement of the quite highly sensitive sample testing in chemistry or other research.

Even though there are already some fluorescence detection systems for the clinical or biomedical applications, the existing fluorescence detection system has the bottleneck problem, with either a low sensitivity or a large-size for the biochemical applications of the portable device/system, LOC and POC. Usually, they do not meet the requirements of the POC testing or the portable system of medicine. Thus, for many reasons, laboratory directors, supervisors, managers, and senior technicians should strongly consider reducing the volume size of the fluorescence detection system to adapt to the portable and miniaturized medical detection equipment, replacing conventional fluorescence detection instrumentation, saving money, and increasing sensitivity. The new device will significantly enhance their professional effectiveness and dramatically reduce technician time per test, further reducing costs.

1.3   Research Objectives

It is imperative to develop an accurate and quantitative diagnostic system for the early stage of cancer or other diseases. Diagnosis and monitoring of complex diseases such as cancers require quantitative detection of multiple proteins. Thus, it is necessary to detect the infectious diseases very early and to do the treatment. To take cancer for example, there is an urgent need to develop a portable detection device and biomedical testing chip for cell detection and POC testing in medicine. In our project, we particularly concentrate on the need of POC diagnosis and detection system.

The main research objective is to develop a cost-effective autonomous microfluidic chip with stop valves and trigger valves for the fluid flow manipulation, and also to develop a portable miniaturized highly sensitive optical detector for the fluorescence detection, which are the two important parts of POC testing equipment.

These devices will be applicable to detect other diseases and proteins based on the available antibody. Regarding the microfluidic devices, the pump and external power supply are usually used to actuate the liquid flow in the microchannels. Usually, the external actuator mechanism makes the system complicated and hard to operate. In order to simplify the system, one possibility is to apply capillary action as a liquid driving force. Liquid passes into the capillary channel only by the capillary action at the gas-air-liquid interface, which is referred to as capillary-driven flow. Some studies have addressed the capillary action as a driving force instead of mechanical or electrical micropumps [18-19].

From capillary theory, we know that the total capillary force or fluidic motion strongly depends on the channel surface condition. If the surface is hydrophilic, the microchannel will generate a large capillary force. Hence, surface treatment is necessary for increasing the capillary force. There are a few publications referring to the chemical plasma coating, the simple hydrophilic coating, and the self-assembling approach to deposit chemicals or molecular layers on the inner surface of the channel to do the surface treatment. In our work, a simple surface modification method for the device cover sheet to characterize the original surface is found.

Then, an autonomous capillary system in microfluidics will be proposed and designed. Such a capillary-driven pumpless system is suitable for a disposable point of care diagnostic system. In order to estimate capillary force in a rectangular channel, it is necessary to obtain the shape of the interface. Although there is some calculation for the interface's shape in a rectangular channel [20], it is difficult to estimate the interface's shape and the capillary force for a general channel's shape with any width and height.

Therefore, simulations were performed and calculations made for our designs. Then the low cost autonomous capillary system on a silicon chip was fabricated for fluid flow manipulation for samples and buffer flows without any external pumps.

Afterwards, this project pursues the specific aim to develop an optical system for fluorescence detection, which is low cost, highly sensitive, and miniaturized. To achieve high sensitivity and miniaturization, the design and the highly efficient fluorescent-based sampling scheme will be considered and designed in detail to enhance the sensitivity of the fluorescence detection. The optical detection device for the fluorescent signal typically consists of a light source for emitting light, an excitation filter to eliminate the unwanted light, a dichroic mirror for the optical separation of excitation and emission channels, and a detector with electronics for signal processing. It should match the requirements of current clinical portable analysis and detection systems.

1.4   Dissertation Outline

Chapter 1 introduces the motivation and some information about this research work and is followed by the objectives of this dissertation. Also, the previous related research work is presented. The research goals and the dissertation organization are shown here.

Chapter 2 overviews the knowledge of portable detection systems and describes the biosensors along with some other analysis detection instrumentations. Also, it gives the basic theories for the capillary action and the CFD-ACE$^+$ simulation results of the running models for the capillary filling and microvalves. In addition, this chapter describes the whole design of the analysis detection system and a wide range of applications as well.

Chapter 3 focuses on the design of the autonomous capillary system with stop valves and trigger valves fabricated on a microchip bonded with a long term hydrophilic surface modified PDMS (PEO-PDMS) as a cover for the utilization in LOC and the micro total analysis system (μTAS) [21]. These kinds of valves are favorable to control the capillary fluid flow well and to perform complex biochemical reactions on the chip, enhancing the features of the whole microfluidic system with a range of functionalities.

Chapter 4 introduces a novel, highly sensitive and miniaturized fluorescence detection system which integrated a LED light source, all necessary optical components, and a photodiode with a preamplifier into one small package, especially for the applications of LOC, portable bio-detection systems, and POC diagnostic systems.

Chapter 5 concludes the experimental results of our research work. There are some improvements, better techniques, and possible future extensions recommended in this section.

CHAPTER 2

BACKGROUND AND DEVICES DESIGN

2.1   Background of Current Portable Optical Detection Devices

POC tests will be widely used because it can help to reduce the length of hospital

stay and improve patient management, which reduces the disease burden and will also

benefit the healthcare system [15]. In light of this, the portable detection and diagnostic

system is generated to meet the requirement for ease of operation in testing. Recently, the

POC diagnostic system has been either too large or has too low of a sensitivity for disease

detection. To overcome these shortcomings, miniaturization is primarily driven by the

need to reduce costs by reducing the consumption of reagents, decreasing analysis times,

increasing efficiency, and enabling automation. Miniaturization of the detection devices

will offer many advantages when rapid and selective monitoring is required. A simple,

portable, and handheld microfluidic device and detector should be developed and should

match POC testing.

One of the technologies to conquer the difficulty of the large size of the detection

system is LOC technology. LOC has numerous applications in the biomedical application

or disease diagnosis because of its small size, low volume requirement for samples, and

rapid analysis. LOC has increasingly developed in integrating the fluid actuation, sample separation, sample pre-treatment, signal amplification, and signal detection into a single device. In addition to diagnosis and sensors, LOC technologies can be utilized to promote the development of therapeutic compositions. The LOC concept is about the fabrication of devices in which all components are miniaturized, including the excitation source, sample preparation, and the fluorescence readout unit. The bodies of these devices are basically made of inorganic (silica) and organic polymers. Some different automatic micro-fabrication techniques, such as embossing, replica, laser ablation, and injection molding are used to produce fluidic channels and the reactive and optical elements [22].

The reduction of the size and the volume of the sensor and chemical reactor devices by several orders of magnitude can be achieved with present technologies. LOC technologies have manipulated the samples and sensed them in a dramatically reduced volume and miniaturization. µTAS and LOC devices have been developed widely in many laboratories and have great potential to improve the current biomedical or clinical diagnostic system [23]. Though there are a number of detection methods utilized together with microfluidic systems, fluorescence is the commonly used method in this area. The rapidly developed technologies allow low cost and miniaturized products of integrated microfluidic systems that incorporate a variety of optical detection elements as light sources and optical detectors. There are miscellaneous sensors integrated into these

devices to be applied in the real practical applications, ranging from small molecules to nanoparticles and intact living cells.

Around the 1990's, microfluidic technologies and LOC have been perceived as having the potential to be powerful applications due to their advantages of their small size, low volume requirement for samples, and accurate analysis. Furthermore, integrating fluid actuation, sample pre-treatment, sample separation, signal detection, and signal amplification into a single device have been developed a great deal [24]. Based on these technologies, currently many bio-detection systems are widely studied, such as the electrochemical method, refractive metrology, fluorescent detection, conductive detection, infrared detection, Raman detection, and mass spectrometry, which are presented in others' papers [25]. But fluorescence-based detection is the most used because of its inherently high sensitivity, selectivity, and efficiency for detection. The fluorescence detection uses a certain wavelength and high energy beam, such as a laser or LED [26-27] to excite unknown sample characters with a fluorescent label. By reading the emitted fluorescent intensity from the labels, the unknown concentration of the sample target per unit volume can be obtained [28]. In order to achieve the high sensitivity, conventional bio-fluorescent systems usually adapt a CCD camera, detection microscopy [29] and photomultiplier tubes, which are expensive and do not match the size of the microchip and portable systems [30], even though they are sensitive. Nevertheless, the diagnostic tools and system can be made compact, miniaturized, less

expensive, and easy to use. Also, they would be especially capable at the point of need, such as emergent diagnosis, so that millions of people would benefit from them. There are some publications available concerning the miniaturized detection system. One of the presented methods used for the portable detection systems integrates optical fiber on a chip to form an excitation light platform for fluorescent light detection with disposable microfluidic chips [28]. Another paper presents a system which integrates a sensor fabricated using the complementary metal oxide semiconductor (CMOS) technology with SU8 lens and a V-shaped inclined mirror and was performed successfully to build a micro-fluorescence detection chip [31-32]. These systems have a low sensitivity because they are difficult to fabricate and integrate all optics on a chip by MEMS technology. Thus, the existing systems are either too large or have a low sensitivity. Controlling the signal to noise ratio is especially hard, and they do not filter the unwanted light, so they are not favorable to the high sensitivity portable detection system. At the present time, only a few research papers reported the miniaturized detection system, which assembled and integrated the optical components found in the commercial market [33-34]. The size of the system is about 5 cm × 5 cm × 5 cm with two 3 cm long tubes, and the sensitivity is about 1.96 nM. As they stand, there is a need to design a miniaturized detection system for the corresponding applications. The miniaturization of medical technologies has the potential to improve public health detection, and perhaps even to change the basic methods by which the patients are diagnosed and treated [35]. This kind of detection

system must be an inexpensive, portable and ideally used compact instrumentation that consumes less power.

2.2   Background of Autonomous Capillary Systems

Microfluidics enables biotechnological processes to proceed on a scale--microns. In the microscale domain, the sample volumes and assay times are reduced, and procedural costs are lowered. Current biomedical and analytical techniques can potentially benefit from an integrated reduction in scale through lowered production and operating costs. Microfluidics technology has essentially taken advantage of the inherent properties of liquids and gases at the microscale and used semiconductor technology in order to build singular miniaturized devices using a streamlined manufacturing process.

During the last two decades microfluidic systems have attracted much interest in various fields, such as chemistry, biology, and medicine [36]. In recent years, they have been widely used in the LOC and μTAS for biochemical analysis applications on biotechnology, drug discovery, and environmental monitoring [37-41]. However, the integration and miniaturization of systems are the big challenges. The concept here is to realize the functions of the bio-laboratory into a Si chip fabricated by photolithography, such as microreactors, mixers, micropumps, and microvalves. The photolithography for micromachining has been commonly applied to miniaturize the chemical, biochemical, and biomedical analysis systems. This kind of microfabrication is a useful method to fabricate the miniaturized devices. Some reports have demonstrated the general

advantages of miniaturized systems, compared with conventional large synthesis devices [42-46]. The miniaturization of these systems has many merits, such as the small volume reagents and/or sample consumption, reliability, automatic performance control, and the portability in the POC, which are beneficial to the biochemical analysis. Currently, the capillary action phenomenon is of great interest in the microfluidic research area because of its simple fluid flow control without extra pumps. Therefore, fluid control devices, such as stop valves have become a main focal research topic in the capillary fluidic system. Many valve schemes have already been presented by now [47]. They can be categorized as either the active or the passive types. The active valve [48] usually contains the closure parts, such as membranes or pistons, and is actuated by pneumatic, thermal or electrokinetic methods. These methods either require an external actuation mechanism, such as piezoelectric, electrostatic, and electromagnetic, or are very sensitive to the physicochemical properties of the components and other factors. These factors usually result in high cost, complexity in integration, difficulty in implementation, and complicated fabrication. The passive valve [49] works using surface tension and the energy balance principle, which has some advantages, such as no external power supply, the possibility of use without an active control, ease of integration, continuity in substrate material, and a low cost. However, the passive valve still strongly depends on the variances in the fabrication process and is not suitable for all of the fluidic mediums. There are two main methods to make the capillary stop valve. One kind is to make the

channel surface hydrophilic and the substrate surface of the valve hydrophobic for the enhancement of the resistance to stop the liquid at the opening of the valve [50]. The other kind of capillary valve does not need an additional process to deposit a hydrophobic coating. It only relies on the surface tension and the static contact angle of the interface of the channel surface and the liquid viscosity [51]. Thus, the control of the burst pressure barrier is dominant over the other parameters in the fluid flow manipulation. A few publications have mentioned its successful utilization in chemical and biological analysis system units [52]. The predetermined volumes of liquid sample to a point of use are precisely delivered by the combination of the capillary filling with stop valves [53-57]. In addition, the cover sheet bonding to the microchip is also critical in the design. At present, the microchip with capillary channels and stop valves often utilizes the glass as the cover. However, it is hard to drill the holes into the glass as the inlets and outlets of the device for testing. Moreover, ordinary glass is usually much more hydrophilic so that the liquid may not stop at the opening of the stop valve, but it is good for liquid flowing fast in the capillary channel. Another cover sheet for the microchip is the widely used ordinary PDMS, which is very hydrophobic (the contact angle is over 102°), and makes the liquid flow slowly and even stop moving forward in the capillary channel sometimes. According to these existing difficulties of designing the effective capillary channel and stop valve, we propose a hydrophilic surface modified PDMS, which is used as the microchip cover. Its contact angle of the PDMS can be adjusted to balance the fluid

flowing in capillary channels as well as to be stably stationary at the valve opening. The long term modified PDMS surface hydrophilic property dramatically simplifies the whole LOC system and enables the fabricated device to be portable and reliable. It is evident that PDMS is simply used in microfabrication and is very important for the domain of microfluidics. This method provides an easy way to design a simple capillary microfluidic system for different applications in biomedical and chemical analysis instruments.

Based on the burst pressure and the surface energy balance principle, a pumpless capillary system with the passive valves will be presented. The testing of the autonomous capillary system in the experiments will be described in the latter section. The principle of the microfluidic chip design is understood by considering a surface energy balance, which is compensated by a great deal of manipulation performed against the Laplace pressure. The type of self-control capillary system designed is pumpless, without external actuators. The passive valves function well depending on the PDMS surface treatment with the PEO surfactant, which can adjust the static contact angle of the PEO-PDMS. In our work, PEO-PDMS will be utilized as the cover of the microchannels to demonstrate capillary-driven flows and common fluidic processes, which could be performed without the use of on-chip or external pump or any powered actuators. This type of capillary stop valve with the modified PDMS can be applied in many different microfluidic based bioanalytical testing, such as cell detection, protein adsorption [58-59], and so on.

2.3   Biosensors and Other Analysis Instrumentations

Biosensors integrate the biological elements into sensors to realize higher selectivity to the substance to be measured in a mixture containing many other substances. Many different biological elements, such as enzymes, antibodies, cells, and tissues have been used in biosensors as well as sensing principles, such as optical, mechanical, electrochemical, and so on. The applications of biosensors are not only limited to biomedical or clinical use but also are extending to other fields of industry such as fermentation control and environmental applications for monitoring pollution. They are analytical tools to analyze the bio-material samples, which gain bio-composition, structure and function by converting a biological response into an electrical signal. There is a biological recognition element directly interfaced to a signal transducer within the analytical devices, and the transducer relates the concentration of an analyte to a measurable response. Therefore, biosensors can measure compounds present in the environment, chemical processes, food, and the human body at a low cost when compared with traditional analytical techniques. However, biosensors are also employed in food analysis. In the food industry, optics coated antibodies is commonly used to detect pathogens and food toxins. The light system in these biosensors usually uses the fluorescence detection method, due to the amplification of the signal and the high sensitivity in this type of the optical measurement, so it is a very common detection method.

There are still many other analytical instruments, such as spectrometers and chromatographs, used to determine the number of chemical species contained in a sample. Various chemical analyzers will be introduced: mass spectrometry, chromatography, electrophoresis, magnetic resonance, and so on. Mass spectrometry is an analytical technique in which atoms or molecules are separated according to their mass. There are some forms of mass analyzer, such as the magnetic sector analyzer, the quadrupole analyzer, the ion trap, the time-of-flight analyzer, and ion cyclotron resonance instruments [12]. Chromatography is an analytical technique in which the components in a mixture are separated based on their differences in speeds of moving or through a column when a gas or liquid is forced to flow through it. The electrophoresis is an analytical method in which the migration of ions in an electric field causes the separation of ions exposed to the field [15]. Magnetic resonance is an analytical technique based on the measurement of absorption of electromagnetic radiation by either electrons or nuclei in the presence of an external magnetic field. The principle of magnetic resonance is a method in which an electron or a nucleus can be regarded as a spinning charged particle [60].

2.4   Capillary-based Microfluidic Device and Detector Design

In this project, an autonomous capillary system, which is based on the control of the capillary burst pressure and adopts surface tension as the driving force without any external actuators, will be designed. The passive valve of the capillary system will be

patterned and fabricated on a silicon wafer and then bonded with the modified PDMS

cover to produce the proposed device. The key point of this proposed design is the change

of the opening angle of the stop valve and the surface contact angle of the modified

PDMS cover of the device so that it will achieve the capillary action and stop valve

function at the same time. PDMS is a popularly used non-toxic and gas permeable

material in microfluidic systems, which is relatively cheap and does not break easily like

glass. The simple fabrication, optical transparency, and elastomeric property make PDMS

a handy material to work with. In order to develop much more different applications of

PDMS in microfluidics and bioengineering, it is necessary to modify the PDMS surface

nature to improve wetting characteristics, and to have a better control in nonspecific

binding of proteins and cells, as well as to increase adhesion. At the moment, the

hydrophilic surface modification performance of PDMS is known to recover its

hydrophobicity soon after oxidation modification, which is not stable in the long term

[61-62]. The PDMS-b-PEO is utilized in this research as a surfactant additive to be added

into the PDMS base and the curing agent mixture during polymerization to create a

hydrophilic PEO-PDMS elastomeric module. The surface of PEO-PDMS can be adjusted

to have different contact angles with the different mixing ratios. The capillary stop valve

in different expansion angles will be tested using red-colored deionized (DI) water as the

testing solution. The concentration of PEO and the contact angle of PEO-PDMS will be

controlled to bring the capillary channel and valve into effect. This type of stop valve can

be used in different applications while changing the valve's open angle or the PEO-PDMS contact angle. The liquid meniscus stops at the opening of the valves in the experiments when the surface tension achieves balance. This stop valve can be widely applied to a number of microfluidic devices and pumpless fluidic actuation mechanisms, which is needed for the cost-effective, diagnostic tools in the biomedical analysis applications. The bonding condition of the modified PDMS to a silicon wafer will also be investigated. This easy bonding method can be widely used in the capillary devices/systems, and microfluidic devices for fluid flow control of the microchannels in the biological, chemical, medical applications.

Afterwards, the capillary stop valve with a trigger valve can be assembled to form the capillary system where two kinds of liquids can meet in the chamber connected with the valves. Figure 2.1 is the shape of our designed autonomous capillary system with a stop valve and a trigger valve. It can be reorganized with other microfluidic parts to generate different devices for the application in microfluidics. Here is the principle of this configuration of the stop valve and the trigger valve. For example, two liquid samples need to be mixed, and then they will flow forward together to the outlet of the device. Thus, we inject the first liquid sample into the capillary system, and then it is pinned at the opening of the stop valve. At this moment, the second liquid sample is introduced from the second inlet to another channel connected with a trigger valve. The second liquid passes through the trigger valve and moves into the chamber. The front of the

second liquid spreads slightly in the chamber and causes the triggering functionality. In some cases, the triggering fails because the liquid from the trigger valve is too far from the stop valve so that the front of the liquid forces the meniscus to be pinned at the opening of the stop valve. Our proposed effective and easy way to control the liquid movement or absorption can be used in microchips, portable miniaturized devices/systems and LOC for biological, chemical, medical applications, mainly for analytical purposes. It also provides a way to design the capillary functional microfluidic device for disposable and portable systems. The trigger valve will be tested by the colored DI water in the latter section.
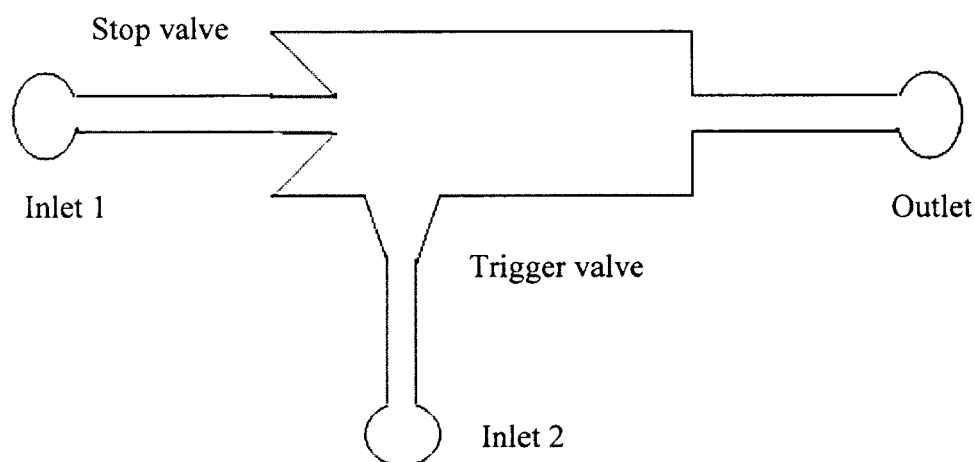
Figure 2.1 The stop valve and trigger valve's pattern design.

A low-cost miniaturized and highly sensitive fluorescence detection system with a built-in amplifier for the LOC applications enables the low molar range measurements under the dark testing area. It will be developed in our research study. In general, optical

systems for the detection of fluorescent signals typically consist of the following components: a light source for emitting light at a suitable wavelength range, an excitation filter to eliminate unwanted light, a dichroic mirror for the optical separation of excitation and emission light path, an emission filter, and a detector with electronics for signal processing. For the past few years, mercury lamps and lasers have been traditionally used as light sources. As they are both bulky and expensive, their combination with LOC devices results in a chip-in-a-lab rather than a LOC. They cannot meet the requirement for the current biomedical applications.

The proposed prototype is a novel, highly sensitive and miniaturized fluorescence detection system which integrated a LED light source, all necessary optical components, and a photodiode with a preamplifier into one package, especially for the applications of LOC, a portable bio-detection system and a POC diagnostic system. The prototype will be tested using the fluorescence dye solution and diluted with DI water as the testing samples. The resolution approximation method is accepted to evaluate sensitivity. It is necessary to develop a cost-effective detection system with a remarkable sensitivity which should meet most of the bio-detection requirements. The system can be widely integrated to the portable device and system for the fluorescent detection in biological, chemical, medical, POC diagnostic applications.

Our proposed capillary system device requires no complex microfabrication strategy. Also, it is very flexible for different microfluidic applications. Figure 2.2 shows

a sketch of the capillary based microfluidic chip design. This device design is based on the shape of Figure 2.1, which can compose different microfludic devices for different requirements in the research studies or other uses. In Figure 2.2, if there are two chemicals solutions A and B needed to be reacted in the microchannels, A can be dropped into the inlet 1, flowing in the capillary channel only with capillary action and then stopped at the opening of the stop valve. Next, the solution B is dropped into the inlet 2 and then pass through the trigger valve to contact the solution A. Thus, the two chemical A and B will move forward together and have enough time to react or mix in the reaction area. Then both of A and B reach the second stop valve and stop at the opening of the valve. At this time, the testing sample (blood or urine sample) is ready to be injected to the inlet 3 and pass through the trigger valve to trigger the solution A and B moving forward together. Finally, they can stay in the detection cell for the fluorescent signal detection with a portable optical detector. The testing liquid sample can be moved outside the testing device through the outlet of the system shown in Figure 2.2. Also, some external mechanism can also be added to the detection part to improve the system which can match different requirements in the microfluidics applications. Thus, this whole system with the portable highly sensitive detector can be widely used in many biomedical or clinical applications. Therefore, this kind of capillary system represents a promising tool for the microfluidic and other biomedical testing applications. Currently, the miniaturization and LOC have played an important role in biomedical applications due to

their high sensitivity, efficiency for detection, and parallelization to a number of bioanalytical platforms. The miniaturized detection device will be beneficial to the miniaturized bioanalytical system and commercial POC diagnostics and detection instruments for the biomedical or environmental testing, which is low-cost and has some safe features for operation.
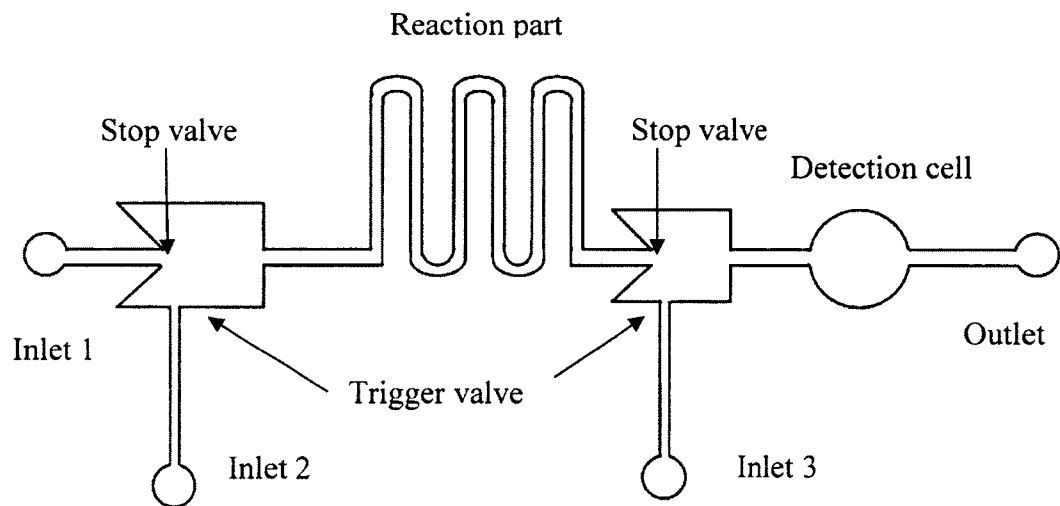
Figure 2.2 The capillary based microfluidic chip design.

CHAPTER 3

CAPILLARY-BASED MICROFLUIDIC CHIP AND PEO-PDMS APPLICATIONS

3.1 Basic Theory and Simulation Results

Many real world problems in engineering and science are solved by complex differential or integral equations in some theories. The solution to a recent particular problem is provided by the solutions to these equations. The Finite Element Method (FEM) is a numerical procedure for obtaining an approximate solution in a reasonable time frame to a variety of problems encountered in engineering analysis areas. CFD-ACE$^+$ (ESI CFD In. 2009) is a commercial finite element software for the simulation of MEMS devices. The advantage of CFD-ACE$^+$, unlike generally used software like ANSYS, ABAQUS, is that it is specially written for MEMS applications, and it has MEMS solvers and material database for MEMS and meets the simulation requirements of the microsystems/MEMS devices designer. MEMS technology has been emerging and developing rapidly in the engineering industry related to many different engineering disciplines and physics: electrical, mechanical, material, chemical, optics, and fluidic engineering disciplines. The microfluidics analysis modeling in CFD-ACE$^+$ is necessary in our research project. The fluid flow in a rectangular microchannel with capillary action and capillary driven stop valves were modeled with a commercial computational fluid

dynamics (CFD) program (CFD-ACE$^+$ 2009, CFD Research Corporation, CA, USA).

Figure 3.1 shows the flow chart for creating a MEMS model in the design.
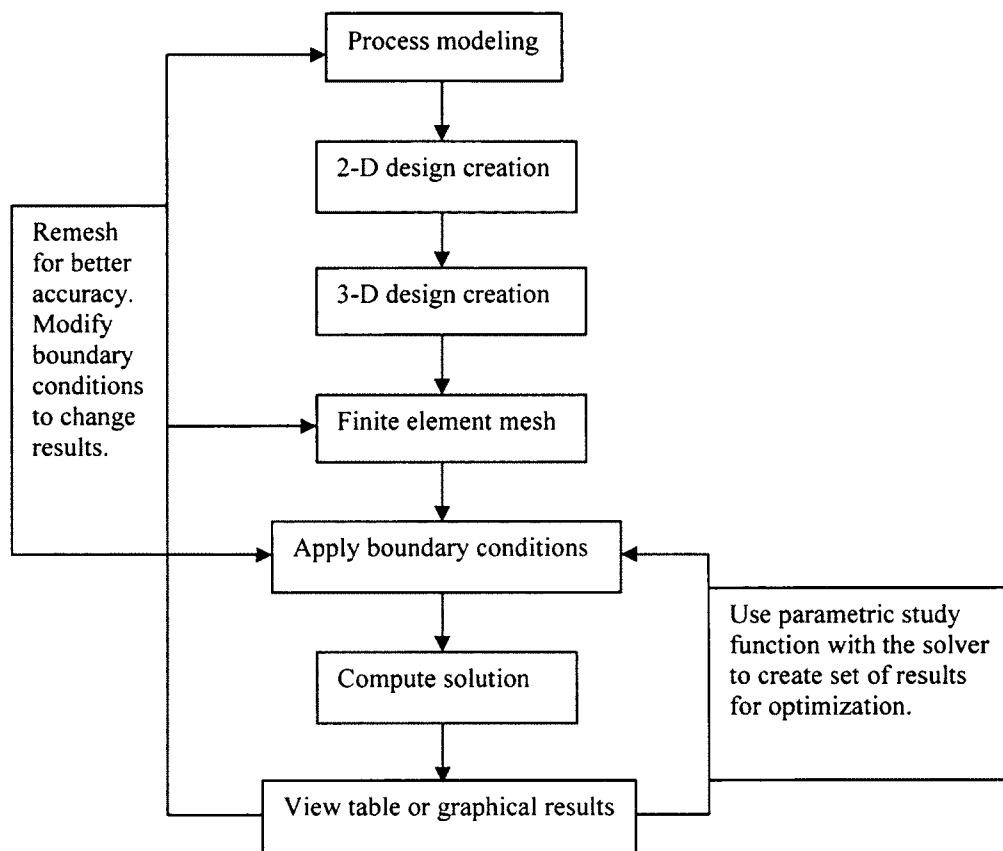
Figure 3.1 Typical design flow chart in software.

Capillary filling is commonly encountered in biochip design and the microfluidic research area. The biochip design usually uses long microchannels to deliver liquid samples from one place to another. Different capillary filling behavior, such as the filling time, or the possibility of entrapping an air bubble may occur due to the different geometry of the liquid flow. Therefore, based on momentum conservation there is a reduced-order model of the filling process derived from it. The agreement of the reduced-order modeling and the simulation results demonstrate the correctness of our modeling.

The model used here is a rectangular microchannel, which is initially filled with liquid (its density is ρ, dynamic viscous coefficient is μ). The microchannel has the width of H, and the height of L_0. The surface tension coefficient σ and contact angle θ can define the contact property between the liquid and channel wall. Usually, passive capillary filling process means that the surface tension force drives the liquid to proceed in the microchannel. The ordinary phenomenon of fluid flow in the microchannel involves the overhead pressure ΔP; here $\Delta P = 0$ is used for our simulation model. In this model, we assume that the liquid height is denoted by L, the average velocity is denoted by u, and the flow time is t. This model uses two-dimensional Poiseuille as the velocity profile. The momentum change can be balanced by surface tension force, pressure overhead (this term is zero for this case) and wall viscous force. The momentum of the liquid column may be written as ρHLu. The momentum conservation equation is expressed as follows:

$$\frac{d}{dt}(\rho HLu) = 2\sigma Cos\theta - \frac{12\mu L}{H}u. \tag{3.1}$$

Noting $u = \dfrac{dL}{dt}$, the equation above can be expressed as:

$$\frac{d^2}{dt^2}L^2 + B\frac{d}{dt}L^2 = A, \tag{3.2}$$

where

$$A = \frac{4\sigma \cos\theta}{\rho H}, B = \frac{12\mu}{\rho H^2}. \tag{3.3}$$

When the liquid column length is L_0, and there is zero velocity, the transient solution can be written thus:

$$L = \left(\frac{A}{B^2} \exp(-Bt) + \frac{A \bullet t}{B} + (L_0^2 - \frac{A}{B^2}) \right)^{1/2}, \tag{3.4}$$

$$u = \frac{A(1 - \exp(-Bt))}{2B \bullet L}, \tag{3.5}$$

here the position of free surface front is L, the time of filling process is t, the average filling velocity of the fluid flow is u. The volume of fluid (VOF) method is used in the simulations of the capillary fluid flows in the patterned-surface microchannels [63]. In this method, the flow is governed by the Navier-Stokes and continuity equations. The fluid flow in the channel is regarded as laminar, operating without gravity, which is ignored in horizontal microdevices, incompressible, and in agreement with Newton's theory.

In the past, researchers have shown that the burst pressure of the geometric capillary system volume is proportional to the surface tension of the liquid and inversely proportional to the channel dimension. However, there is still no further rigorous theoretical development, which can determine the empirical constants appearing in their empirical relationship for the maximum pressure difference that the valve can withstand [64]. Therefore, here we mainly focus on the fundamental working principle of the capillary system. Considering the capillary driven stop valve, initially, the meniscus is seen stopping at the valve edge, and the liquid is at rest. Hence, it is necessary to derive and assess the valve burst pressure and evaluate the valve's ability to stop the capillary flow without external driving pressure. At equilibrium, the partial wetting conditions are applicable in our case. Laplace and Young's equations define the capillary free surface phenomenon [65]. The Laplace equation specifies the pressure drop ($\Delta p = p_l - p_g$) at the

liquid-gas interface. The Young equation presents the relationship of the solid-liquid, liquid-gas and gas-solid surface tensions, which are denoted as γ_{sl}, γ_{lg}, and γ_{gs}, respectively. The contact angle at the solid-liquid-gas triple line is denoted by θ_c, the expression of Young's equation is as follows:

$$\gamma_{sl} + \gamma_{lg} \cos \theta_c = \gamma_{gs} . \tag{3.6}$$
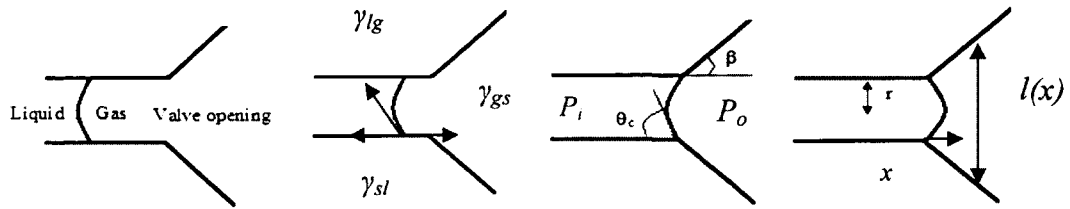
Figure 3.2 Illustration of a meniscus proceeding forward in a capillary channel.

Figure 3.2 shows the shape of the stop valve and also illustrates that the liquid reaches the capillary valve, connecting with a sudden enlargement of the microchannel. Also, the meniscus is pinned at the stop valve edge. The analytical equation of the capillary pressure is written as [51]:

$$P = -\frac{\delta E_t}{\delta V_l} = \gamma_{lg} \left(\cos\theta_c \frac{\delta A_{sl}}{\delta V_l} - \frac{\delta A_{lg}}{\delta V_l} \right). \tag{3.7}$$

Here, E_t is the total interfacial energy of the capillary system, and V_l is the volume of the liquid in the capillary channels. γ_{lg} is the liquid-gas surface tension, A_{lg} is the area of the liquid-gas interface, and A_{sl} is the area of the solid-liquid interface. When P is positive, the liquid flows forward and wets the entire channel surface while a negative opposing pressure can be accomplished by an abrupt enlargement in the channel cross section. This sudden change of the channel makes A_{lg} increase more than A_{sl} for a fixed

volume. Once P becomes negative, the fluid is pinned at the wedge of the valve. The maximum pressure barrier ΔP is expressed as below to stop the fluid flow:

$$\Delta P = \frac{\gamma_{\lg}}{r}\left(\frac{\cos\theta_c - \dfrac{\alpha}{\sin\alpha}\sin\beta}{\cos\beta + \dfrac{\sin\beta}{\sin\alpha}\left[\dfrac{\alpha}{\sin\alpha} - \cos\alpha\right]}\right). \qquad (3.8)$$

Here, r is the radius, $\alpha = \pi/2 - \theta_c$, and β is the expanding angle of the stop valve, which is shown in Figure 3.2. If $\beta = \alpha$, the capillary pressure P will reach the critical wedge angle threshold at zero. The meniscus curvature is also zero. At this point, the capillary system reaches the critical state.

The above analytical expressions are based on the capillary tube, and the expanding angle is 360° around at the circumference of the tube, which are presented by Gliere and Delattre [65]. For the practical microfabrication process, it is impossible to make microchannels similar to this type of round tube, because they are fabricated on a planar microfluidic silicon chip. Therefore, the capillary in a silicon substrate is a rectangular microchannel. For a rectangular capillary, the analytical equation of the capillary pressure can be written as [61]:

$$\Delta P_r = P_i - P_o = -2\gamma\left(\frac{\cos\theta_a}{w} + \frac{\cos\theta_b}{h}\right), \qquad (3.9)$$

where ΔP_r is the pressure difference between the pressure inside the liquid (P_i) and outside the liquid (P_o), γ is the surface tension, and w and h are the width and the height of the channel, respectively. The advancing contact angle θ_a is with the sidewall and θ_b is with the top or the bottom walls.

In our case, the capillary channel is rectangular, and the top of the device is PEO-PDMS cover. Assume that the liquid advancing contact angle with the sidewall and the

bottom walls (silicon substrate) is denoted by θ_s, and with the top is denoted by θ_p. The surface tension of the liquid with the modified PDMS is denoted by γ_{pl}. Then the equation (3.9) can be written as:

$$\Delta P_r = P_i - P_o = -\left(2\gamma_{sl}\frac{\cos\theta_s}{w} + \gamma_{sl}\frac{\cos\theta_s}{h} + \gamma_{pl}\frac{\cos\theta_p}{h} \right). \tag{3.10}$$

Once ΔP_r reaches zero, the liquid meniscus stops instantly because the pressure difference is at balance. The contact angle at which the liquid meniscus starts to move is termed as the critical advancing contact angle, θ_c. If the liquid advancing contact angle of the PEO-PDMS decreases, the whole pressure difference will increase so that it is favorable to the liquid moving forward in the capillary channel. When the stop valve bursts, the liquid interface moves along the diverging sidewall of the valve chamber. The pressure difference in the valve region, can be written by:

$$\Delta P_{ps}(x) = P_i - P_o = -\left(2\gamma_{sl}\frac{\cos\theta_r}{l(x)} + \gamma_{sl}\frac{\cos\theta_r}{h} + \gamma_{pl}\frac{\cos\theta_c}{h} \right), \tag{3.11}$$

where $l(x)$ denotes the width of the stop valve's diverging section in Figure 2.2. θ_r is the contact angle in the rectangular microchannel (between $\theta_c + \beta$ and 180°). Also, θ_p has been replaced by θ_c. Figure 3.3 shows that the pressure has a curved profile depending on the location of the liquid meniscus. Additionally, the cover sheet is the PEO-PDMS with 0.8% PEO concentration inside. If the pressure difference achieves the threshold value, the meniscus will be pinned at the opening of the valve. Once the pressure reaches the burst pressure, the meniscus moves forward into the valve chamber, which is the required lower pressure for the latter movement. Thus, in order to implement the liquid control in the capillary system for different applications, the aspect ratio (h to w) of the capillary channel pattern and the contact angle (θ_p) of the PEO-PDMS can be changed to better

control the velocity of the fluid flow in the capillary microchannel and stop valve. Since

the contact angle (θ_p) of the modified PEO-PDMS can be change from 80.9° to 21.5°

with different PDMS-b-PEO concentrations, this new device provides an effective way to

design and control the flow in the capillary system for a wide range of applications. The

detailed experimental data and analysis will be presented in the next chapter.

The theoretical pressure versus the meniscus location
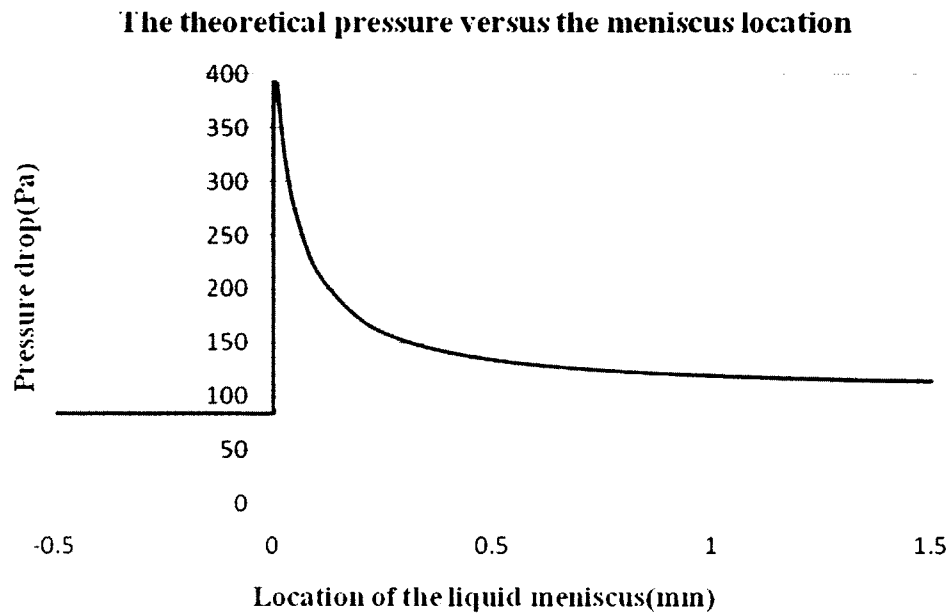
Figure 3.3 The pressure drops greatly once the pressure bursts from the valve opening. The dimensions of the channel and valve fabricated on a Si wafer are such that $w = 30$ μm, $h = 230$ μm and $\beta = 130°$.

Hence, the simulations have been done, and the results obtained will be presented

in the later paragraphs. In the simulation of the fluid flow in the capillary channel part,

the software CFD-ACE⁺ modules were used to do the simulations. Here, the fluid flow in

the rectangular channels with only capillary action was modeled in CFD. The simulation

model was performed under several different conditions, such as different sizes of the

channels corresponding to different contact angles in the microfluidic flows. The

different channel widths, such as 75 μm, 100 μm, 150 μm, and 200 μm were simulated, and the same lengths of 1600 μm were used in every case, with the same depths of 10 μm used in every case. Each of them corresponds to the different contact angles, such as 60, 70, 90, and 100 degrees. Almost 20 sample points were observed during 0.002 seconds to generate the curves of velocity versus time. Then the relationship between the velocity and the channel size was concluded as well as the contact angle. According to the simulation values, several curves were obtained as follows. The wider the channel width, the smaller the velocity with the same contact angle. Basically, the velocity goes down with the increase of the contact angle whatever the channel width is. Then based on the theory and modeling results, our channel layout pattern was designed to continue the microfluidic part of our research project. Figures 3.4, 3.5, 3.6, and 3.7 illustrate the curves for the velocities of the different widths of the channels, such as 75μm, 100μm, 150 μm, and 200 μm under the different contact angles, such as 60, 70, 90, and 100 degrees. The following figures 3.8, 3.9, and 3.10 are the shapes of the meniscus profile of the liquid in the 100 μm width 1000 μm length microchannel under the different contact angles, such as 60, 70, and 90 degrees. Figures 3.11, 3.12, 3.13, and 3.14 indicated the different flow position of the different widths of the channels, such as 100μm, 200 μm, 300 μm, and 400 μm at the same time under the same contact angle of 60 degree. It shows that the larger the width of the channel, the slower the fluid moves. Figures 3.15 and 3.16 show the velocity versus the width of the channels with different contact angles at the same running time. They show that the velocities will decrease when the widths of the channels get bigger. From these curves in Figure 3.17, it indicates that the velocity of the fluid flow decreases with the increase of the contact angle.

Contact Angle: 60-degree
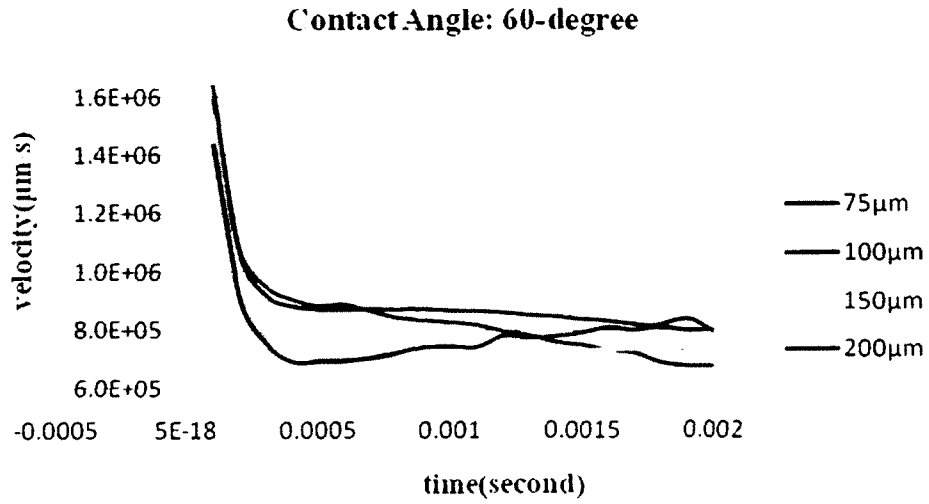
Figure 3.4 The velocity versus time at the contact angle of 60°.

Contact Angle: 70-degree
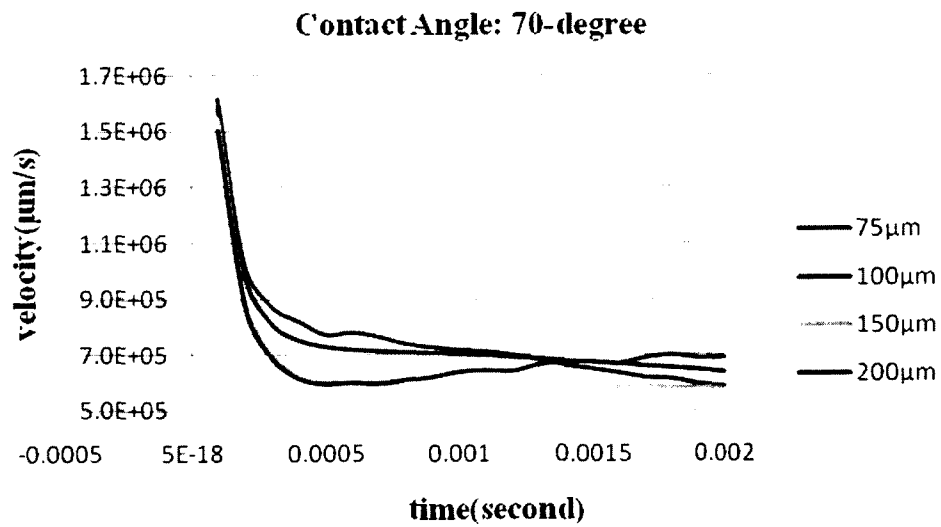
Figure 3.5 The velocity versus time at the contact angle of 70°.

Contact Angle: 90-degree
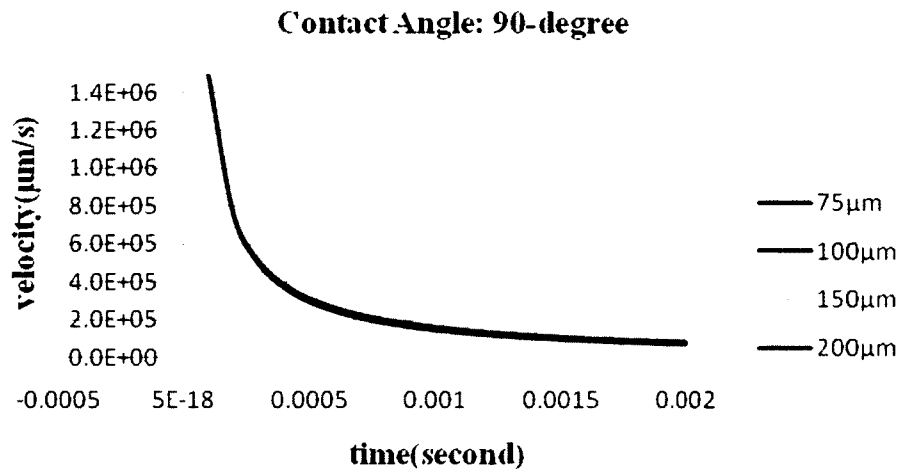
Figure 3.6 The velocity versus time at the contact angle of 90°.

Contace Angle: 100-degree
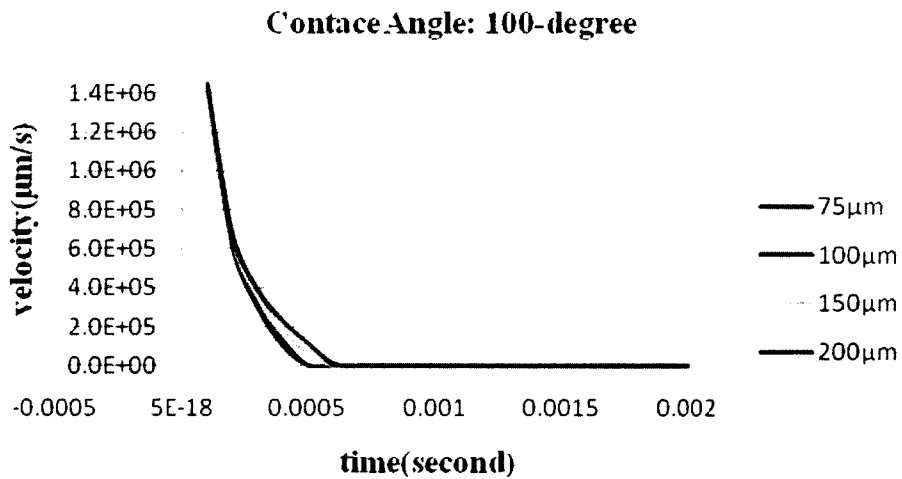
Figure 3.7 The velocity versus time at the contact angle of 100°.

Figure 3.8 The liquid meniscus location (the contact angle is 60°).

Figure 3.9 The liquid meniscus location (the contact angle is 70°).

Figure 3.10 The liquid meniscus location (the contact angle is 90°).
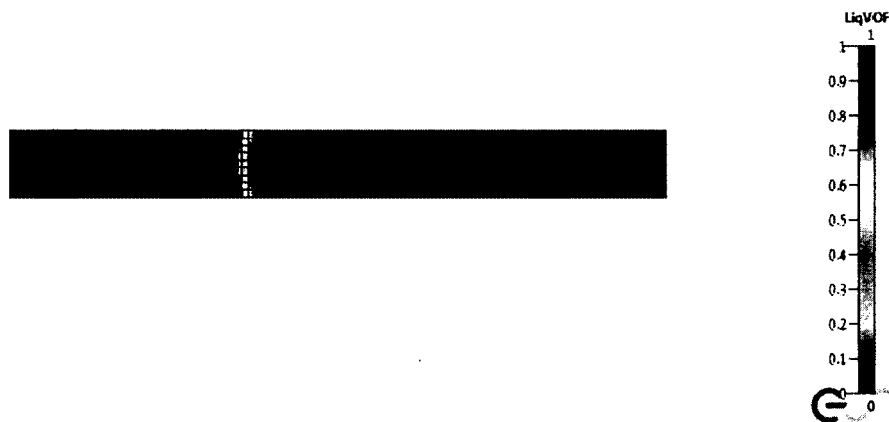
Figure 3.11 The width of the capillary channel is 100 μm.

Figure 3.12 The width of the capillary channel is 200 μm.

Figure 3.13 The width of the capillary channel is 300 μm.

Figure 3.14 The width of the capillary channel is 400 μm.

Contact Angle: 40-degree at 0.0004s
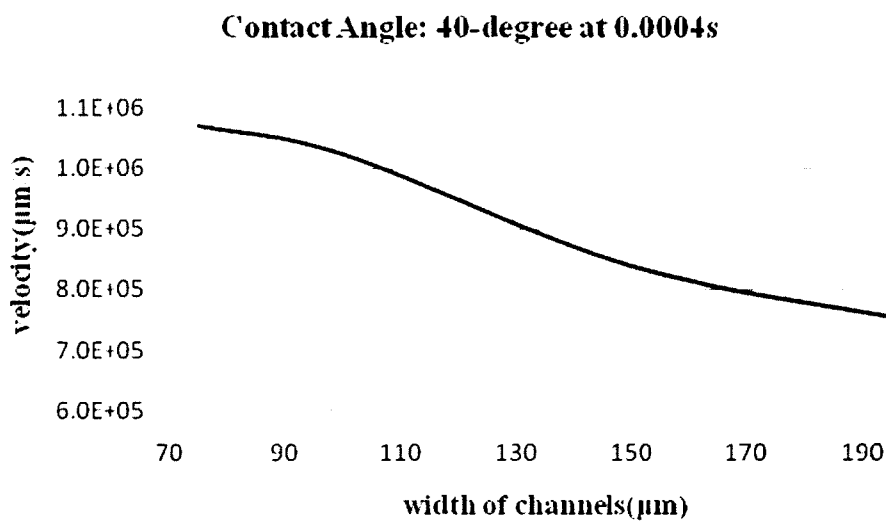
Figure 3.15 The velocity versus the width of the channel with the same contact angle of 40° at the same running time.

Contact Angle: 60-degree at 0.0004s
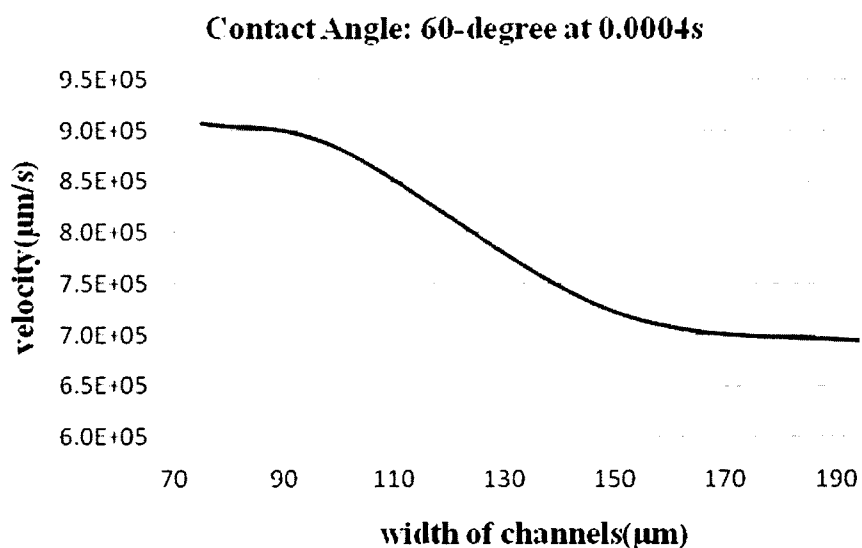
Figure 3.16 The velocity versus the width of the channel with the same contact angle of 60° at the same running time.

Time: at 0.0004s
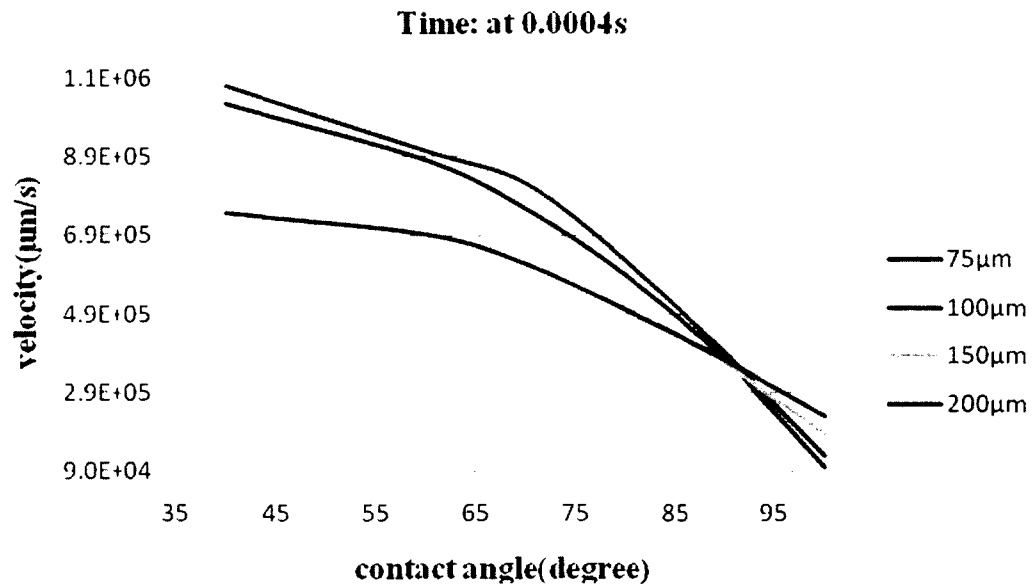
Figure 3.17 The velocities versus the different contact angles.

Regarding the simulation of the stop valve part, CFD-ACE+ software was used to simulate the modeling. Fluid properties of the microchannels have also been investigated by means of computational fluid dynamic (CFD) simulation to validate the criteria of the capillary action channel design. Then the CFD software was utilized to describe the phenomenon of the fluid flow in the channel and at the opening of the stop valve considered in this work. The channel was considered to be fully wet, then the different contact angles were specified on all the other walls. The passive capillary filling process was regarded as a constant pressure (atmospheric) set at the channel inlet. A liquid volume fraction (LiqVOF) unity value was used in this module. Here, the pressures at the channel inlet and outlet were specified at zero for all cases. The numerical technique of this part is shown below. The channel geometry was created and meshed using CFD-GEOM modeler (ESI CFD Inc., 2007). CFD-ACE[+] in CFD software based on the finite volume method is used for the time dependent simulations. The flow and free surface

modules of CFD-ACE$^+$ were used for data analysis. An automatic time step option automatically ensures the stability in the CFD-ACE$^+$ solver. After all the parameters were set up and the designed model was run, some results of our experimental simulation were obtained.

Here, the fluid flows were simulated in the microchannel of 300 μm long and 100 μm wide, which is connected with a stop valve. Different sizes of the capillary-driven valve with adjustments of the geometry of the opening of the valve were designed. Figures 3.18, 3.19, and 3.20 show the cases of different contact angles with the same expansion angle of the valve at 45°. Changing of the contact angle generates different effects of the stop valve and different meniscus positions in the chamber. It is shown that the larger the opening of the valve, the better the valve's effect which means that the liquid easier to stop at the opening of the valve and also stay for long time. In addition, the bigger the contact angle, the better the valve's effect with the same size of the valve. In comparing Figure 3.18 with Figure 3.21, the simulated illustrations show that the larger the valve's expansion angle, the better the valve's effect. These results and conclusions will be the guide for our latter practical fabrication of the stop valve.
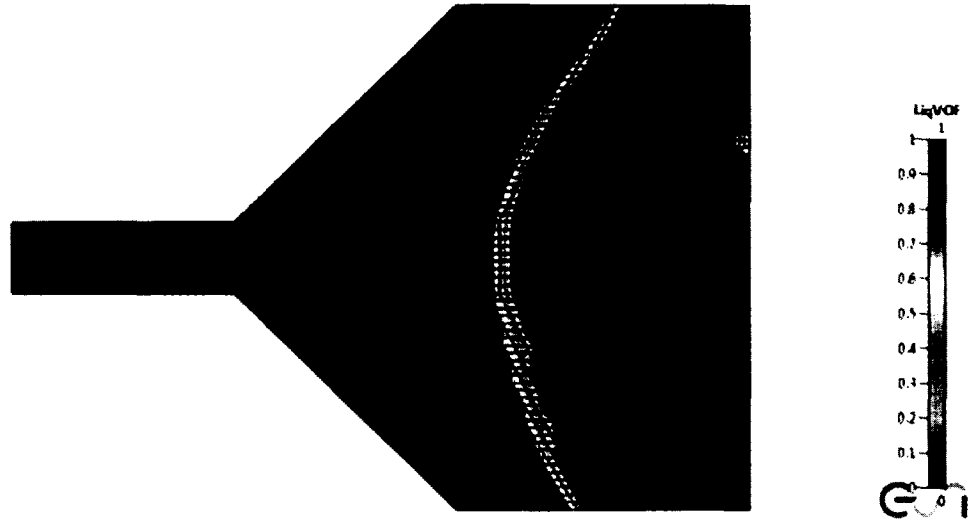
Figure 3.18 The liquid meniscus movement in the stop valve (the contact angle is 60°).
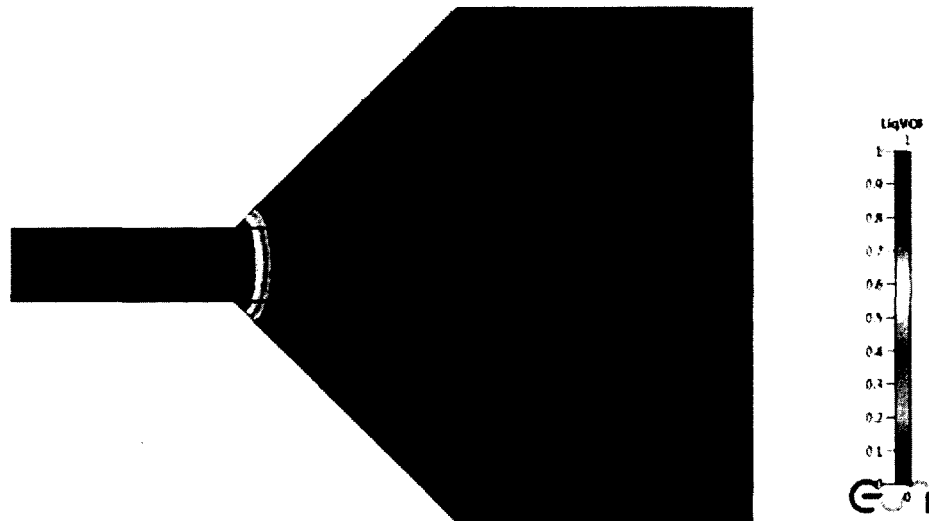
Figure 3.19 The liquid meniscus movement in the stop valve (the contact angle is 70°).
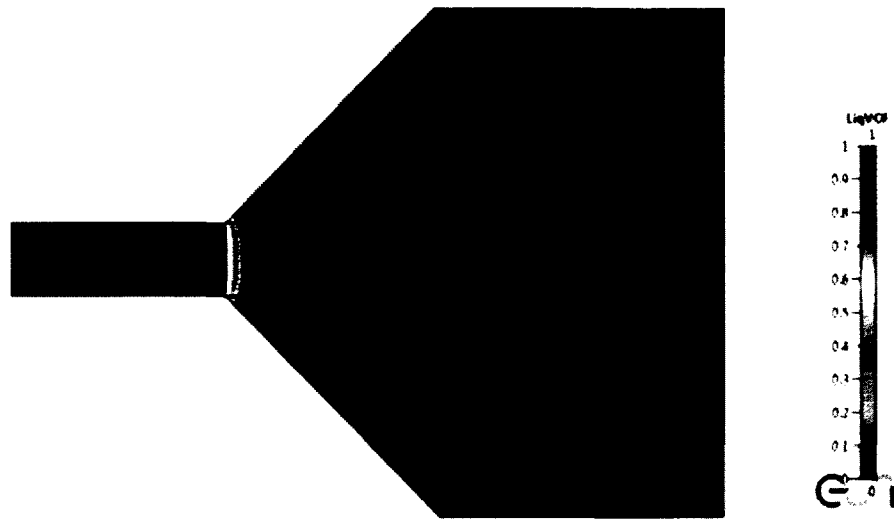
Figure 3.20 The liquid meniscus movement in the stop valve (the contact angle is 80°).

Figure 3.21 The liquid meniscus movement in the stop valve (the contact angle is 60°, the expansion angle of the stop valve is 80°).

3.2   Current Status of PDMS Surface Treatment

PDMS is a non-toxic silicon-based organic polymeric material, and it is widely used in microfluidic systems. The hydrophobic surface of PDMS becomes hydrophilic after the oxygen plasma treatment under certain process conditions. It is favorable for the liquid sample flowing through the microchannels on the Si wafer [66]. However, the

hydrophobicity of the ordinary PDMS is the big limitation, which is unfavorable for some applications, such as protein adhesion, cell engineering, and capillary fluid functional microchannels, because the untreated PDMS is very hydrophobic (the water contact angle is around 103°), although it has many merits, such as low cost, widespread availability and ease of fabrication. Thus, in our research the ordinary PDMS cannot make the self-pumping capillary system function well, so a durable PDMS surface hydrophilic modification method will be proposed to adjust the contact angle of the PDMS. It is found that the modified PDMS is relatively simply used in microfabrication and at a low cost in comparison to other materials (e.g., glass or silicon). Since the rapid development of MEMS technology in recent years, there has been already a great deal of research published on this topic. One commonly used approach for generating the hydrophilic PDMS surface is its exposure to an air or oxygen plasma [67]. The oxygen is used as a reactive gas (40 ~ 50 sccm), the radio-frequency (RF) power is controlled in the range of 350 ~ 400 W. However, the result under this kind of treatment is temporary, and the surface will recover to hydrophobicity within a few hours [68-69] because plasma treatments do not change the mechanical properties of the bulk materials. Besides, there are some other PDMS hydrophilic surface modification strategies, such as the physical coating approach, including physisorption of charged amphiphilic polymers and copolymers [70-71], and the chemical assembled monolayer approach, such as layer by layer deposition, sol-gel coatings, silanization, dynamic modification with surfactants, and protein adsorption [72]. In addition, these treatments are long and complicated fabrication processes with inaccessible or expensive machinery. They dramatically alter the bulk PDMS properties and/or lack long term surface stability. They may also lose a

good PDMS property, which can be easily bonded on Si/SiO$_2$ wafer. The dynamic coating involves the surfactants and ionic liquids to modify the PDMS surface to hydrophilicity, which simplifies the technique. There are some other publications [73-74] which present the method for the preparation of hydrophilic elastomers involving the synthesis of PDMS with tunable hydrophilic surface properties. This method combines the PEO surfactant additive with a PDMS base and curing agent during polymerization to create the desired hydrophilic properties of PDMS elastomers. The hydrophilic balance is controlled by changing the surfactant chain segment lengths. Another general approach to modify the surface property of PDMS is the electrostatic layer-by-layer (LbL) self-assembly technique, which has been developed to coat the ultrathin hydrophilic membrane or nanometer thick films on any surface [75-77]. This technique alternately applies positively charged polymers (polycations) and negatively charged polymers (polyanions) onto a charged surface whose film thickness of each monolayer is approximately from 1 nm to 6 nm for most polyions [78]. The surface modified PDMS after hydrophilization has been used in applications, such as biomolecule separations, enzyme microreactors, immunoassays, and cell culture studies. The emergence of spatially controlled immobilization of biomolecules or cells, inside PDMS microchannels, has a high trajectory of innovation in regard to bioanalytical endeavors and tissue engineering.

The PDMS-b-PEO has a hydrophilic property to be commonly used as a surfactant additive. Han et al. [79] reported the use of immobilizing PDMS-b-PEO molecules on the PDMS surface and demonstrated the increased hydrophilicity of the PDMS surface by a swelling-deswelling process. A low cost and one step bulk mixing

method with PDMS-b-PEO to modify the surface hydrophilic property will be proposed in the latter section. The modification of the PDMS hydrophilic surface is appropriate for the fluid passing through the microchannels. This hydrophilic PEO-PDMS surface has many benefits for the fluid flow in the microchannels because the contact angle is adjustable. This kind of PDMS surface modification technique can also be applied in the nonspecific protein adsorption, soft lithography [80], and microfluidic large scale integration [81].

3.3   Preparation and Fabrication of PEO-PDMS

The PDMS is ordered in two separate bottles. One bottle is the primer, and the other one is the curing agent. The blending ratio between a primer and a curing agent is usually 10:1. In the process, it is necessary to place aluminum foil onto the work surface and the balance to cover and keep them clean, also, wear gloves because the viscous liquid can be messy. The PDMS-b-PEO surfactant additive is chosen to hydrophilize the PDMS surface in this experiment. The general formula of the polymeric surfactant PDMS-b-PEO is presented in Figure 3.22. This applicable polymeric surfactant additive may be a linear or branched polymer. It is comprised of a hydrophobic segment, or anchor, which is compatible with the base elastomer (e.g. PDMS) and serves to solubilize the additive within the elastomer matrix during preparation, and later serves to anchor the additive in the cured PDMS. The additive is also comprised of hydrophilic pendant chains, which impart desirable surface properties to the formed elastomer monolith, where van der Waals forces interact in the PDMS base polymers. Then the polymeric surfactant additive is sufficient to lead to a stable hydrophilic surface. Further, the extent of surface modification of PDMS monoliths may also be tuned by varying the molecular

weight of the polymeric surfactant additive and/or the ratio and/or the configuration of the hydrophobic anchor to hydrophilic pendant chains. In addition to modifying the surface energy of the PDMS monolith, the optical properties of the formed PDMS monoliths can be tuned by varying factors, such as the concentration, molecular weight, configuration, and hydrophobic/hydrophilic balance of the polymer additives.

$$H_2C-CH_2-CH_2-(O-CH_2-CH_2)_x-O-CH_3$$
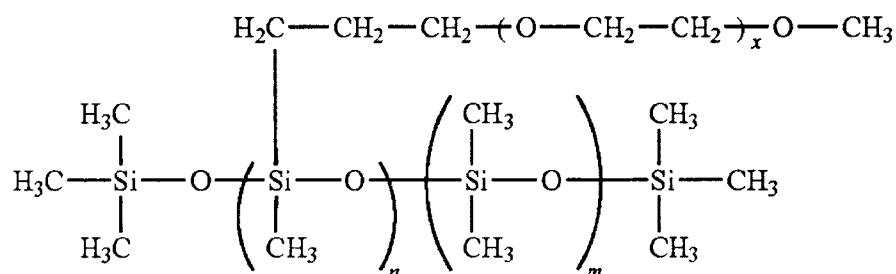
Figure 3.22 The general formula of the poly(dimethylsiloxane-b-ethylene oxide).

The materials for the experiments, Sylgard®184, an elastomer PDMS kit, is purchased from Dow Corning Corporation and contains two chemical parts: a PDMS polymer base and a curing agent. Block copolymers of PDMS-b-PEO are purchased mainly from Polysciences Incorporation, which has a PEO branch molecular weight of 600 and the viscosity of 20 cps. All of these chemicals are transparent, but quite viscous in nature. Using pipettes is not recommended to draw the chemicals, as they are very thick. Also, wearing gloves is necessary when handling these chemicals. The PEO-PDMS is prepared by mixing the PDMS prepolymer base, the curing agent, and PDMS-b-PEO copolymer in a ratio of 100:10:1.0 (or 1.3, 1.5, 1.7, and 1.9). Among these chemicals, the PDMS-b-PEO copolymer is the surfactant additive to modify the PDMS surface, which exhibits hydrophilicity. Finally, the three chemicals are mixed completely and evenly. The mixture is degassed for 30 ~ 40 minutes in a vacuum (0.06 MPa) to remove bubbles

[61], and it is subsequently put into an oven for baking at 70°C ~ 80°C for approximately 1.5 hours. After that, the cured PEO-PDMS can be peeled from the container and the static water contact angle can be measured with the portion. The results obtained will be discussed in the next section. The completed PEO-PDMS is used as the cover for the microchannel fabricated on the Si wafer. However, the bonding of PEO-PDMS to Si wafer is a critical part for the application here. Thus, different processes attempt to bond PEO-PDMS onto the Si wafer after the RF oxygen plasma treatment with Technics Micro-RIE Series 800 plasma system. Eventually, the optimum bonding parameters are obtained, which can be found in the later part of this paper. The bonding parameters tried are quite effective for bonding PEO-PDMS with the Si wafer, which facilitate the fluid flow in the capillary channels and the injection of the liquid into the channels on the chip, enhancing the capillary effect.

The PEO-PDMS of different concentration mixtures are made by the concentrations of 1.0%, 1.3%, 1.5%, 1.7%, and 1.9% (the percentage to PDMS base polymer in weight). The hydrophilic PEO-PDMS monoliths are successfully prepared by incorporating a small amount of PDMS-b-PEO block copolymer to a PDMS polymer base and a curing agent with a one simple step mixing method, which is indicated in Figure 3.23. The method for the preparation of hydrophilic elastomers involves the synthesis of PDMS with tunable hydrophilic surface properties. The PDMS-b-PEO surfactant additive chain segment lengths are varied to control the hydrophobic/hydrophilic balance. Regular PDMS surfaces with tethered PEO block copolymers exhibit a dynamic surface where wettability changes very rapidly, maintaining long term stability. However, most of the recent hydrophilic surface

modification methods are usually short term, and involve quick hydrophobic recovery after surface hydrophilization, which are not favorable to the microfluidic movements.
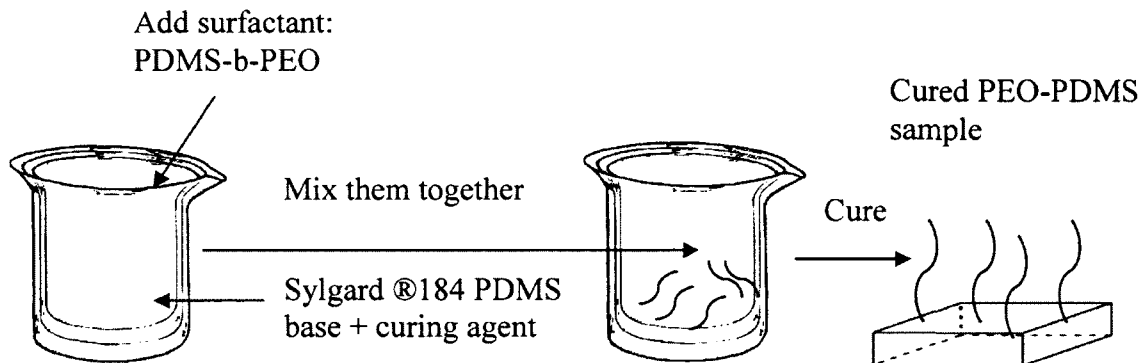
Figure 3.23 Fabrication of PEO-PDMS.

3.4 Design and Fabrication of Capillary Stop Valves and Trigger Valves

The fabrication of the microfluidic chip with the autonomous capillary system should be performed in a clean room. The designed devices are fabricated in a single crystal silicon wafer (100 mm diameter, 500 μm thick) with a 0.6 μm thick silicon oxide layer. The patterns of the channels, stop valves and trigger valves on the wafer are fabricated by the standard photolithography process associated with the buffered oxide wet etching (BOE) and inductively coupled plasma (ICP) dry etching [82]. In the beginning, the wafer is placed on a hot plate for about half an hour at 250°C for the hard bake. After the wafer is cooled, an approximate 2 μm thick photoresist is spin-coated on it. The wafer is then soft baked at 90°C for one minute. The mask aligner machine MA6 will be used to transfer the pattern of the capillary channel and the stop valve from the mask to the photoresist by ultraviolet (UV) light. Then it is developed in a microposit MF-319 developer solution to define the distinct pattern. After that, it is cleaned with DI water and blown dry to bake at 115°C for one minute. These above steps are performed

on the SiO_2 layer. The photoresist layer is used as an etching mask, and the SiO_2 layer is etched in a BOE solution. After BOE etching, ICP dry etching is used to etch 230 μm deep channels and valves in the silicon. Here, the standard Bosch process [83-84] is applied, which makes high aspect ratio silicon structures with vertical sidewalls possible [85]. Finally, the low pressure SF_6 plasma generated by a RF source is used to clean the C_4F_8 deposition layer on the substrate and the walls of the channel and the valve. Due to these fabrication processes, the substrate and sidewalls of the pattern are smoother and more hydrophilic than the one without SF_6 plasma cleaning. We performed all the microfluidic chip fabrications in the clean room, a class-100 clean room, which is often used as a work place for microfabrication. The clean room is a work area with a controlled temperature and humidity to protect sensitive equipment from contamination of air borne particles. It is usually built with plastic walls and ceilings, external lighting, with a continuous intake of clean, particle free air.

The PDMS cover applied here is a surface modified hydrophilic PEO-PDMS, and the process of the PEO-PDMS preparation has been presented in the previous section. Then, the silicon chip and PEO-PDMS are finally bonded together. Also, the surface of the PEO-PDMS is hydrophilic and favorable for the liquid flowing through the microchannels on the Si wafer [86]. Therefore, the PEO-PDMS is used to seal the fabricated device. The fabricated stop valve is shown in Figure 3.24. Each chip has five capillary channels and six valves in different configurations. Additionally, the profiles of the capillary channel and the stop valve are observed by scanning electron micrographs (SEM) in Figure 3.25. Figure 3.26 shows the autonomous capillary system with a stop valve on the left of the chip and a trigger valve in the bottom, and the SEM pictures are

shown in Figure 3.27. The etching depths are measured by a KLA tencor profilometer

(TENCOR Alpha step 500 profiler; TENCOR Inc.) with a precision of ±0.01 μm.
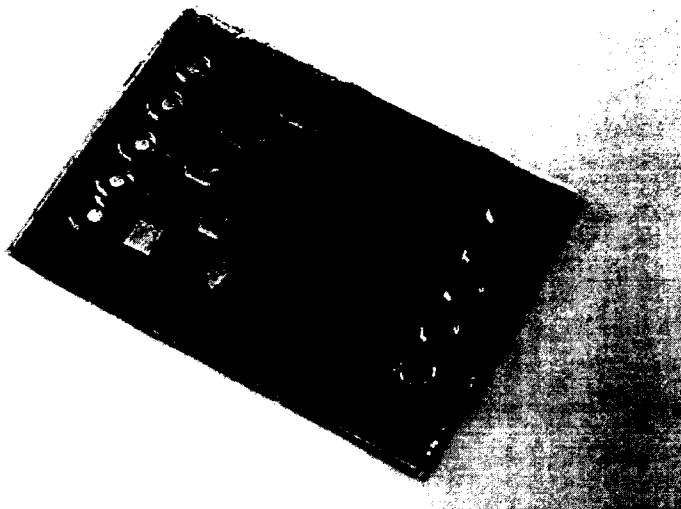
Figure 3.24 The capillary channels and microvales patterns are fabricated on a chip.

(a)

(b)
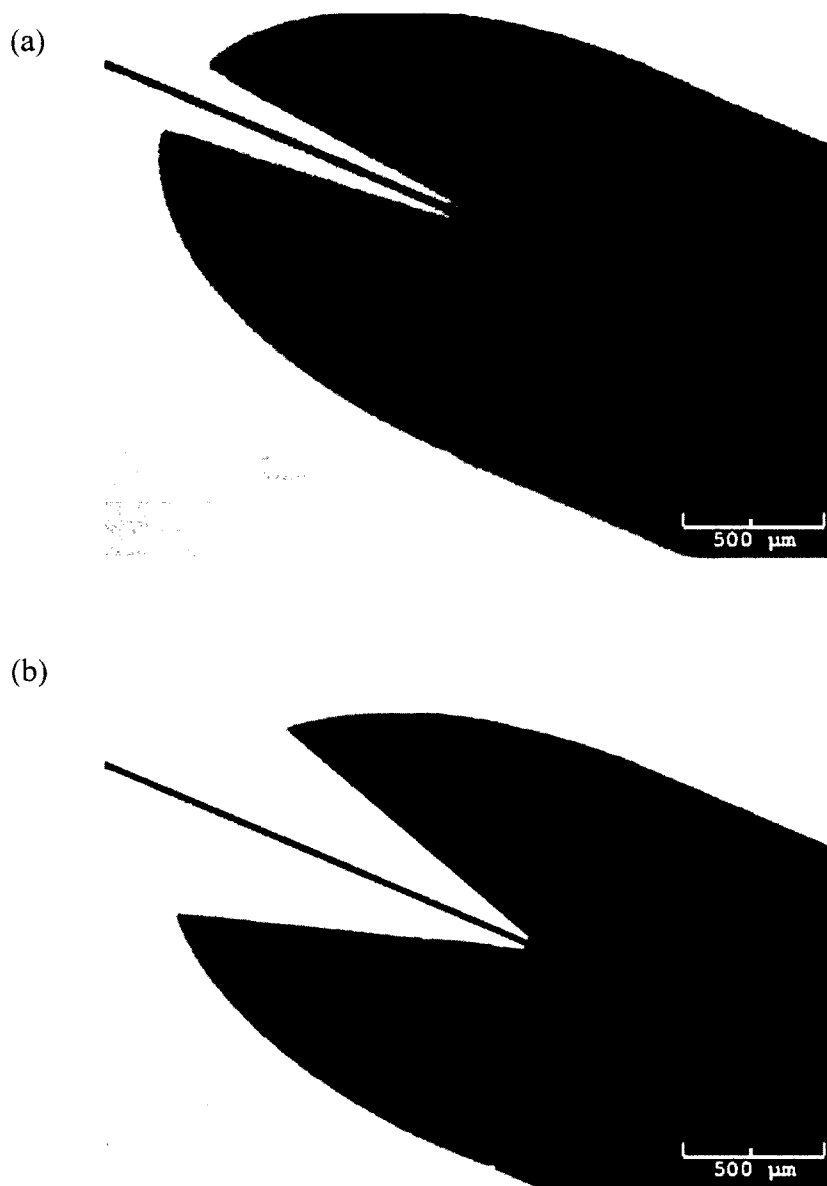
Figure 3.25 SEM images of the etched capillary channels and stop valves. (a) The expansion angle of the stop valve is 170°. (b) The expansion angle of the stop valve is 150°.

(a)
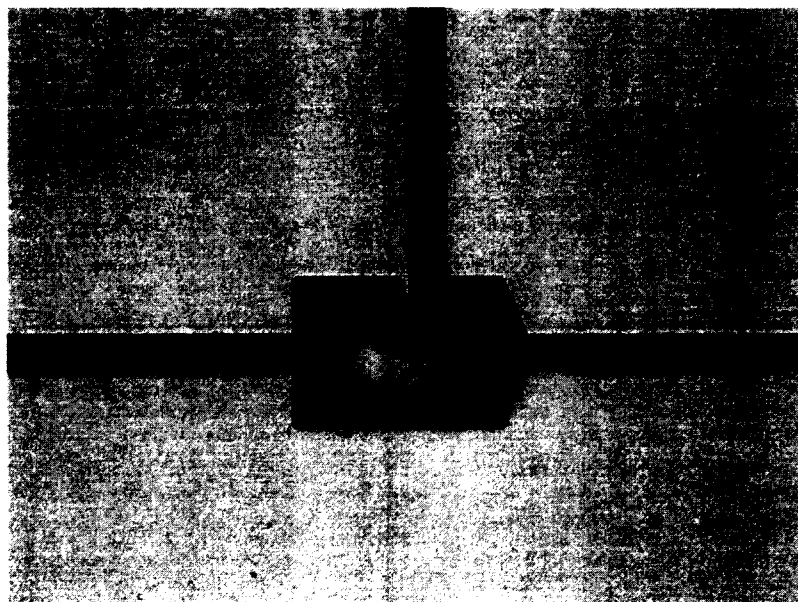
(b)

Figure 3.26 The pictures are taken under a microscope, revealing the capillary system with a stop valve and a trigger valve, fabricated on a Si chip. (a) The stop valve on the left, the trigger valve in the bottom. (b) The stop valve on the top, the trigger valve on the right.
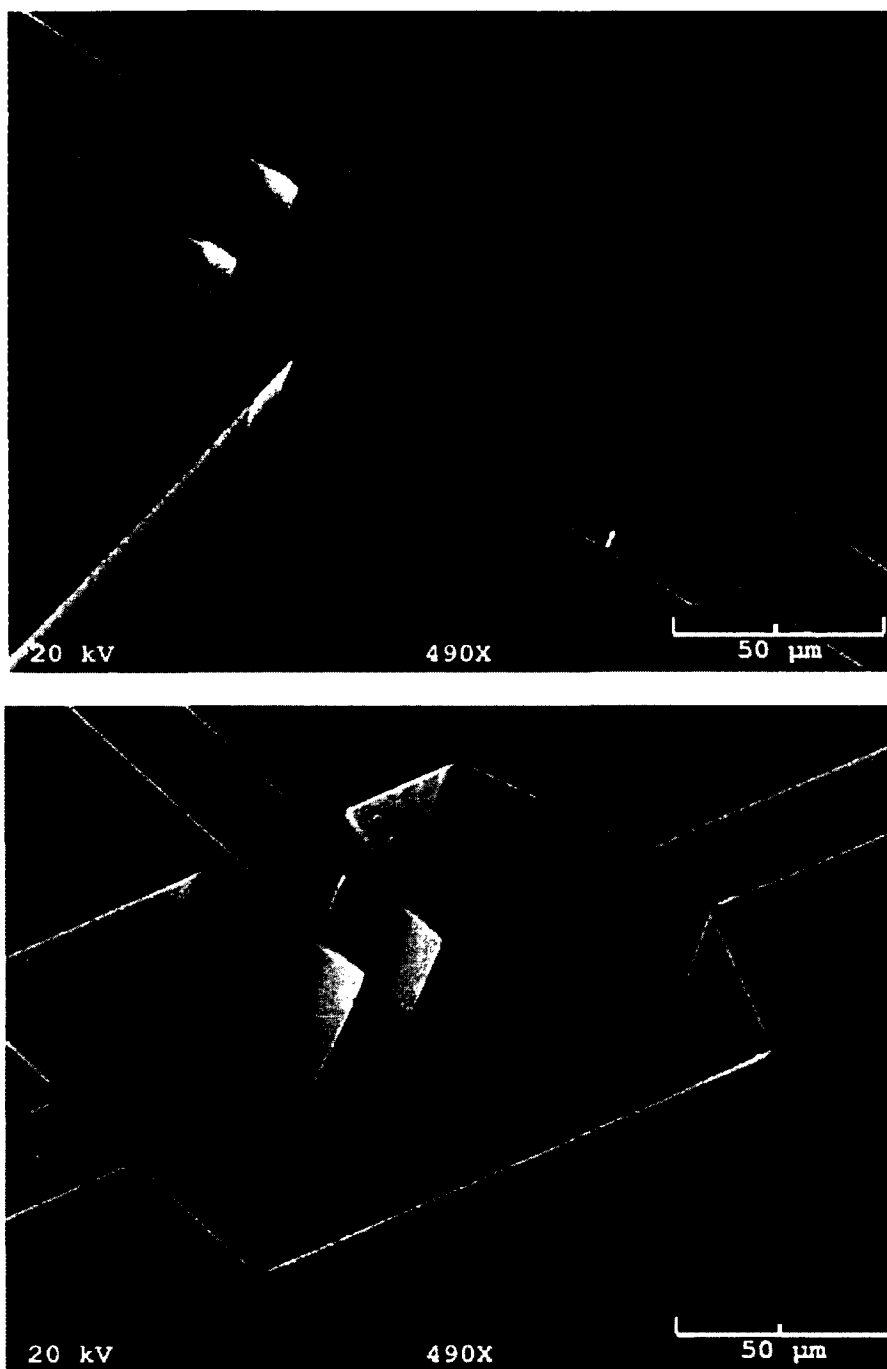
Figure 3.27 SEM images of the fabricated capillary channel with a stop valve and trigger valve profiles (corresponding to Figure 3.5(a) & (b)).

3.5   Experimental Results and Analysis

In our experiment, the fabrication of the PEO-PDMS is one of the main parts, which changes the contact angle of the PDMS in order to control and balance the fluid flow in the microchannel and valve. Previously, we have tried the glass and the original PDMS bonded onto the fabricated Si wafer, respectively. But the glass is too hydrophilic to enable the valve function well, and the original PDMS is too hydrophobic to make the fluid flow stop in the capillary channel. Thus, the hydrophilic PDMS modification is proposed to control the contact angle of the interface and better control the surface tension inside the device. The hydrophilic PEO-PDMS monoliths can be successfully prepared by incorporating a small amount of PDMS-b-PEO block copolymer to a PDMS polymer base and the curing agent with a simple one step mixing method. This method was mentioned by Dhruv [87]. The PDMS-b-PEO is a surfactant additive in the PDMS hydrophilic surface treatment. The method of preparing the hydrophilic elastomers involves the synthesis of PDMS with tunable hydrophilic surface properties. The PDMS-b-PEO surfactant additive chain segment lengths are varied to control the hydrophobic/hydrophilic balance. Regular PDMS surfaces with tethered PEO block copolymers exhibit a dynamic surface where the wettability changes very rapidly. In this study, various PEO-PDMS mixtures are made with the different PDMS-b-PEO concentrations from 0.2% to 1.9% (the percentage to the PDMS base polymer in weight). In order to investigate the hydrophilic property of the PEO-PDMS, the contact angles are measured. One droplet of the DI water with 1 µL is dispensed on the PEO-PDMS surface, and the static contact angles are measured by an OCA40 contact angle meter and contour analysis system. Figure 3.28 plots the curves of the contact angles with different

mixing ratios of PEO (the PEO concentration is from 0% to 1.9%). After 200 seconds, the contact angle will be stable. Compared to the contact angle of 102° for the unmodified PDMS, the modified PDMS markedly improves the hydrophilic property. Figure 3.29 shows the stability of the static water contact angle behavior on the modified PDMS surfaces with the PEO additive. Notably, the contact angle is stable for two months and then slightly changes in the next two more months, according to the curve in Figure 3.8. After that, the contact angle of the modified PDMS surface increases with time.
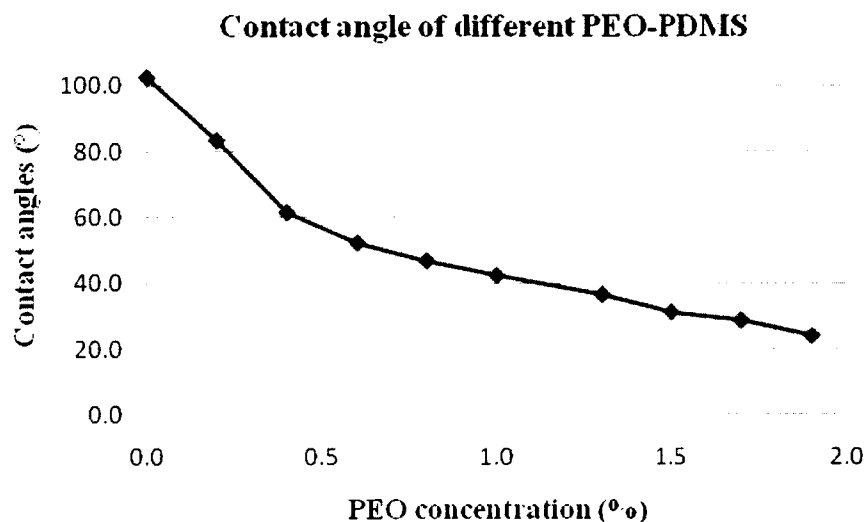
Figure 3.28 Static water contact angles of the PEO-PDMS (the PEO concentration is 0.2% ~ 1.9% to the PDMS base polymer).

**Variations in Contact Angles of Modified PDMS
with 1.7% PEO**
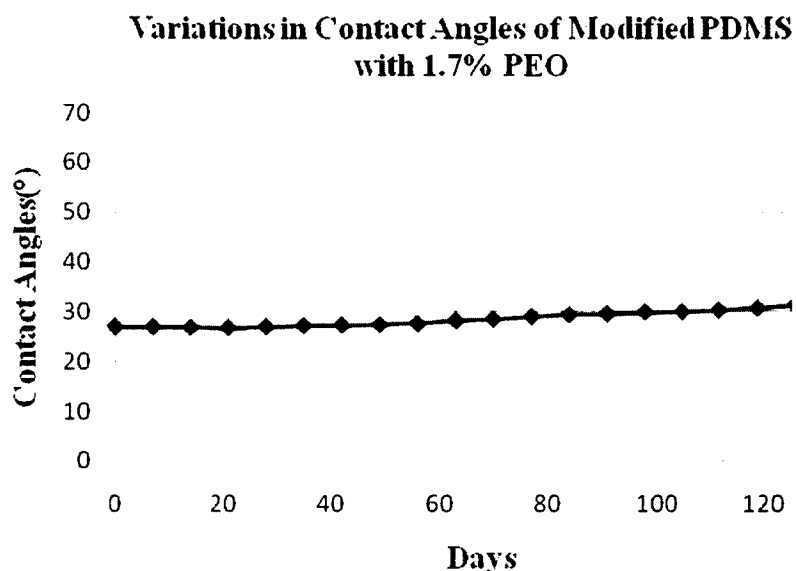
Figure 3.29 The curves are the days versus contact angles, which illustrate the stability
of the PEO-PDMS hydrophilicity.

Then the PEO-PDMS bonding with the Si wafer and glass substrate were studied.

When bonding the PEO-PDMS to a Si wafer, both of their surfaces require much more

rigorous treatments than the original PDMS. For surface modification, the sample of

PEO-PDMS and SiO_2 wafer are placed into the equipment of Technics Micro RIE Series

800 plasma system. A variety of treatment parameters have been set up for the different

testing operations. It is found that the efficacy of the oxygen plasma is critically

dependent on the plasma flow rate, RF power, reactive time, and the concentration of

PEO in the PEO-PDMS. Table 3.1 shows the different bonding strength efficacy with

different parameters when the PEO concentrations are at 1.0%, 1.3%, 1.5%, 1.7%, and

1.9%, while the PDMS with the PEO concentrations at 2.0% or over 2.0% cannot be

bonded to Si wafers and glass substrates. From these tables, we can see PEO-PDMS

cannot be bonded onto the silicon wafer or glass wafer if the PEO concentration is over

2.0%. The best bonding for the low PEO concentration (1.0% to 1.9%) can be achieved

after 15 seconds of the oxygen plasma treatment under oxygen flow at 5 sccm, the RF

power at 50 W, and chamber pressure at 200 mTorr. For the enhancement of bonding

strength, the bonded PEO-PDMS and Si wafer can be heated for 40 to 50 minutes at 90°C

on a hot plate. Afterwards, the testing of fluid flow in the capillary channel will be done

in the latter experiments.

Table 3.1 The bonding condition of the PEO-PDMS (with the concentration of PDMS-b-
PEO at 1.0%, 1.3%, 1.5%, 1.7%, 1.9%) bonding onto Si and glass wafers.

Time (s)	RF power (W)	Oxygen flow (SCCM)	Bonding Efficacy (Si substrate)	Bonding Efficacy (Glass substrate)
15	50	5	Excellent	Excellent
10	50	10	Good	Good
20	50	5	Not bad	Not bad
Over 20 or less than 10	50	10	Bad	Bad

As for the investigation of the fluid flow and the measurement of the liquid flow

velocity in the capillary channel, a capillary channel with 200 μm in depth, 100 μm in

width, and 28 mm in length is fabricated on a Si wafer and bonded with the PEO-PDMS

(PEO concentration at 1.5%, 1.7%, and 1.9%) cover. After that, this device can be used

for testing. The velocities of the fluid flow in the channel are recorded by an i-SPEED 2

high speed video camera, which is an invaluable tool for general research and

development requirements, with recording rates of up to 33,000 fps and instant playback

analysis. Finally, the testing results are obtained and the fluid flow velocities are listed in

Table 3.2, which indicate that the higher the concentration of PEO in the PEO-PDMS

cover sheet, the faster the fluid flows in the capillary channel. Also, it is indicated that

when the PEO concentrations are more than 0.8%, the velocities increase dramatically in the capillary channels. Here, we take the different concentrations for testing in comparison with the different velocities to verify that the contact angles will affect the fluid flow in the capillary channels.

Table 3.2 The fluid flow in the capillary channel (100 μm wide, 28 mm long) with different velocities due to the different PEO-PDMS of different contact angles.

Concentrations of PDMS-b-PEO	Contact angles(degree) at t=200 seconds	Velocity(μm/s)
0	106.5	0
0.2%	80.9	83.4
0.4%	58.5	540.9
0.6%	50.3	980.5
0.8%	43.8	4800.8
1.0%	35.7	8552.7
1.3%	32.9	9002.3
1.5%	30.6	9458.9
1.7%	26.8	9971.5
1.9%	21.5	10139.6

The capillary stop valve and trigger valve are fabricated in a Si wafer and have a size of 230 μm in depth and 15 μm in width. However, there are six different expanding angles of stop valves, including 60°, 90°, 110°, 130°, 150°, and 170° on a chip (Figure 3.3). Then, this chip is bonded with the PEO-PDMS, which has different concentrations of PEO. The red-colored DI water is used as the testing sample solution. After these preparations, the sample liquid is dropped into the inlet by a pipette, and then auto-injected into the capillary channel. Finally, we observe the phenomenon of the fluid flow inside the capillary channel and valve. Table 3.3 lists the stationary time of the liquid at the opening of the stop valve corresponding to different stop valve sizes when the PEO concentration is 0.4%. A detailed explanation can be found in Gliere and Delattre's paper

[88]. Table 3.4 gives the results that the higher the concentration of the PEO, the shorter the time the liquid stays at the opening of the stop valve. Table 3.5 shows that the different aspect ratios influence the fluid stationary time at the opening of the capillary valve, which agrees with the theory of stop valve mentioned before. Table 3.5 and Table 3.6 also give the velocities of the fluid flow in the capillary channels with different aspect ratios and bonded with the same PEO-PDMS, which will result in different velocities. From the data, it is obvious that the lower the aspect ratio, the faster the fluid flows in the microchannels. Because the contact angle of the PEO-PDMS with 0.4% PEO concentration is 58.5°, which is much lower than that of the Si wafer (about 90°), the contact angle of the PEO-PDMS cover is dominant over the bottom substrate and the other two sidewalls of silicon in the microchannel. Thus, the aspect ratio will impact the fluid meniscus stationary time at the edge of the stop valve, which is listed in detail in Tables 3.5 and 3.6. We can see that the higher the aspect ratio, the longer the time the fluid flow is pinned at the opening of the stop valve. Therefore, the stop valve functions very well in this case of high aspect ratio. Figure 3.9 is a picture taken under a microscope and shows the liquid sample stops at the opening of the stop valve. From these data, we can find that the testing results coincide with the theoretical prediction: the bigger the expansion angle of the stop valve, the longer the stationary time will be. The lower the contact angle of the PEO-PDMS, the faster the fluid flows in the capillary channels. The stationary time in this experiment can be greater than 30 minutes until the DI water dries completely when the expansion angle of the stop valve is 170° and the concentration of PEO is 0.2% or 0.4%. However, the stop valve with the 170° expansion angle will not work perfectly when the contact angle of the PEO-PDMS is less than 45°.

The fluid flow holding time at the opening of the valve is important when one reagent sample mixes with another one. It can provide enough time for the two or more different reagents to mix or react in the chamber, so that the fluid flow can resume its advance in the channel for the next step's motion.

Table 3.3 The fluid stationary time for the stop valves with six different expansion angles and the PEO-PDMS cover at the 0.4% PEO concentration.

Capillary stop valve expansion angles	Stationary time
60°	0
90°	0
110°	2 minutes
130°	4 minutes
150°	15 minutes
170°	More than 40 minutes

Table 3.4 The fluid stationary time for the stop valves with the same 170° expansion angle and the PEO-PDMS covers at five different PEO concentrations.

Concentrations of PEO	Contact angles of PEO-PDMS(degree)	Stationary time
0.2%	80.5	More than 40 minutes
0.4%	71.8	More than 40 minutes
0.6%	61.9	15 minutes
0.8%	52.7	5 minutes
>1.0%	< 45.3	0

Table 3.5 The velocities are the fluid flow in the capillary channels with different sizes. The fluid stationary time is for the stop valves with the same 170° expansion angle and the same depth of 100 μm, but the valve has three different aspect ratios of the patterns. The PEO-PDMS cover is at the 0.4% PEO concentration.

Widths of the capillary channels (μm)	Velocity(μm/s)	Stationary time
50	79.7	32 minutes
100	120.4	28 minutes
150	435.8	15 minutes

Table 3.6 The velocities are the fluid flow in the capillary channels with different sizes. The fluid stationary time is for the stop valves with the same 170° expansion angle and the same width of 100 μm, but the valve has three different aspect ratios of the patterns. The PEO-PDMS cover is at the 0.4% PEO concentration.

Depths of the capillary channels (μm)	Velocity(μm/s)	Stationary time
50	329.6	8 seconds
100	120.4	28 minutes
150	19.5	35 minutes

The liquid meniscus locates at this line.

The liquid meniscus locates at this line.

The liquid meniscus stops at this line.
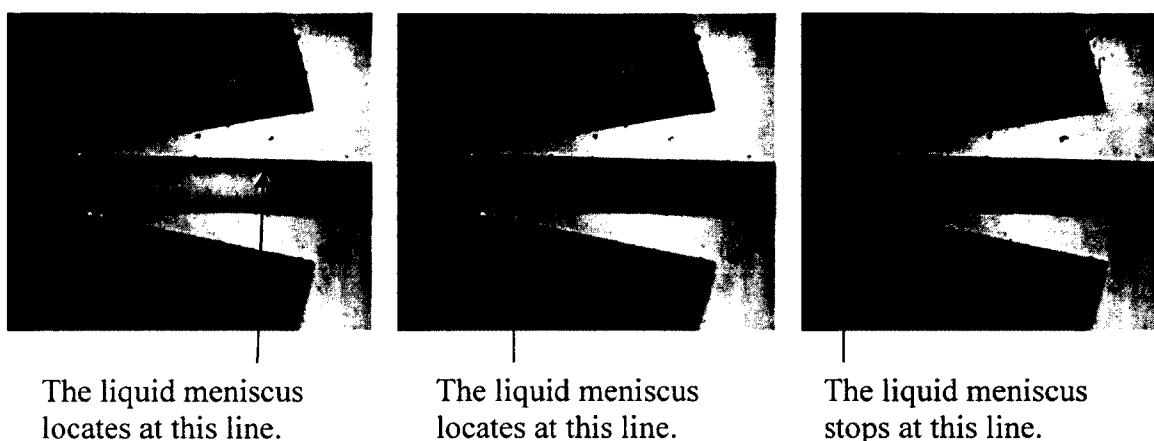
Figure 3.30 Each picture shows different position of the liquid meniscus at different time in the capillary channel and eventually stops at the edge of the capillary-driven stop valve (the colored DI water is the testing sample). Each capillary channel is 230 μm deep, 20 μm wide, connecting to a stop valve of an expanding angle at 170°.

We also found if the PEO concentrations are 1.0% ~ 1.9%, the capillary action works well, but the microvalve does not work. However, if the PEO concentrations are 0.2% ~ 0.8%, the fluid can still flow smoothly in the microchannel with the capillary action, and the microvalve functions well. Finally, the fluid successfully stops at the opening of the valve. But the flow rate may be slower than the higher concentrations of PEO. These results indicate that the surface tension at the stop valve must achieve balance in order to make both the capillary action and stop valve work well. The testing

results are also presented in detail under the different designs: the aspect ratio from 2 to 0.67, the valve expanding angle from 60° to 170°, and the contact angle of PEO-PDMS from 21.9° to 80.9°. The adjustable surface tension of PEO-PDMS and the aspect ratio of the microchannel provide an effective method to control this balance for different applications. This phenomenon can be used for some biochemical applications, such as completely mixing and reacting, etc. As we know, this designed microvalve sealed with the modified PDMS cover has not been published before. All the experimental data will be good references for designers. Currently, there are many other studies describing the phenomenon of the fluid flow in the capillary channel and stop valve considered in this work. Our proposed design and method are easily fabricated and sealed, as well as beneficial to a wide range of biomedical analysis testing systems in related fields.

CHAPTER 4

HIGHLY SENSITIVE AND MINIATURIZED OPTICAL DEVICE
FOR FLUORESCENCE DETECTION

4.1   Introduction to Fluorescence Detection

Recently in biosciences, fluorescence has become popular in the use of biosensors. Fluorescence is the emission of light from a substance that absorbs a beam of light or other electromagnetic radiation of a different wavelength to emit a different light with a different wavelength. This type of fluorescence is produced once a certain dye is illuminated by a kind of light source with a short wavelength. At this point, the compact and miniature design of the whole fluorescence detection system is a major bottleneck blocking many biotechnological assays and other biomedical diagnostic requirements in portable LOC system research. Many of the biological tests and analyses being performed today are based on the principle of fluorescence. As a result, there is a great deal of research in the field of fluorescence detection systems. A typical fluorescence instrument consists of an excitation source and a detection unit.

In the fluorescence detection field, fluorescence lifetime is very important for the real operation system. The methods for measuring fluorescence lifetimes include two kinds, which are frequency-resolved and time-resolved. The frequency-resolved methods typically apply sine wave modulation at a high frequency to modulate the intensity,

67

which can be also called phase-modulation techniques. If the fluorescence sample is excited by a modulated light, the emission signal will respond at the same modulation frequency. However, there is a time and phase delay related to the lifetime of the sample, which is compared to the excitation signal. This time delay is used to calculate the fluorescence lifetime which is characterized by a phase shift. Besides, the intensity of the demodulated signal can also be employed to measure the fluorescence lifetime. The possibility of measuring a short lifetime relies on the frequency of the modulation and the efficiency of the measurement of electrons. The lifetime is also important in the testing of fluorescence. Thus, the experiments should be completed in limited time periods to ensure accurate results. These experiments involve the excitation of molecules with a narrow pulse of light and the measurement of the time it takes for a fluorophore to relax to the ground state following the excitation. The intensity decay is recorded with a high-speed detection system, which permits measurements on the nanosecond timescale.

Hence, the steady-state type is simply an average of the time-dependent intensity decay of the sample. Whereas nanosecond time-resolved measurements usually need complex instrumentation, they provide abundant information at the molecular level, which otherwise would be lost during the time-averaging process of steady-state measurements. The difference in the fluorescence decay time of fluorescent dyes provides a powerful discrimination feature to distinguish molecules of interest from background or other species. Moreover, the fluorescecnce lifetime value is a sensitive reporter of several physical and chemical properties, both of the molecule and its environment. The time-resolved fluorophore is excited by a pulsed light source at a relatively high repetition rate. The time duration of the light pulse should be as short as

possible because the fluorescence lifetime is limited. Thus, the time of the light pulse preferably needs to be much shorter than the fluorescence lifetime measured. The excitation pulse from which the fluorescence lifetime can be determined is time correlated to the emitted photons from the testing samples.

Usually, fluorescence has a variety of applications in the areas of biology and medicine due to its high sensitivity and accuracy. A simple chemical reaction can label the biological molecules with a fluorescent chemical group. Then the fluorescence label of the molecule takes effect in the sensitivity and quantity detection. This type of method can also be utilized in DNA extraction [89], food assay [90], protein detection [91], etc. Due to the split of emission and excitation lights through their different wavelengths caused by the Stokes Shift [92], there are many fluorescence detection methods, such as the laser confocal scanning technique and some other techniques. Almost all of these methods are either bulky or high power consumption. For example, the CCD-based biochip reader is a high-sensitivity method commonly used in DNA detection and medical research but not low volume [93]. However, the current widely used detection devices in the laboratories or hospitals are very large. Thus, this existing method does not meet the need of the utilization in portable, POC diagnosis or personal home-healthcare applications. The use of optical fibre guiding emission and excitation light from the light source to the analytes and then to the detector is another optical detection approach in the biomedical detection system.

4.2   Current Optical Detection with Microfluidic Applications

Presently, there are two ways to realize the fluorescence detection in microfluidic devices. One way contains an integrated optical chip and the microfluidic device part

separated from each other. This makes the microfluidic part disposable and the optical part reusable. For instance, one of the suggested devices [88] consisted of a semiconductor LED, a silicone photodiode, and a CdS optical filter integrated in one unit and a microfluidic reactor located in a close ambient position. In microfluidic parts, capillary action is a simple way to pump fluids in a LOC device because the liquid flows spontaneously with no external power or moving parts. However, the operated vacuum pump can also be used to actuate fluid flow in the field [94-95], which is much more difficult to handle and not easy to operate. The other way is to integrate all the elements that are necessary for efficient instrument performance into one chip. These elements consist of the chemical modification, sample separation, and binding of immobilized sensor molecules with visualization of the result by the essential fluorescence detection technique. In this configuration, the microfluidic units comprise the true μTAS that would be independent of interfacing to external macro-scale equipment. The LOC systems basically miniaturize the structures and integrate several different components assembled on one substrate. They demonstrate three main roles of microchip technologies, which are optics, electronics, and fluidics [96].

Usually, the optically based chemical sensors are commonly used in the chemical or biological analysis. Actually, spectrophotometric techniques have been widely used in analysis, which utilizes the interaction between electromagnetic radiation and molecules, ions, or atoms. Among all these detection and analysis methods, the fluorescence based sensors are popular in the area of biochemistry and biomedicine due to their high sensitivity and accuracy. Usually, each testing sample costs much money and time. Millions of people might benefit from it in some case and certain constraints in medicine

might be conquered when the medical diagnostic tools could be miniaturized, made simple to use and much cheaper, also readily available at the POC, such as emergency diagnosis.

The design and fabrication of the micro-biosensor and chemical sensors are based on microfabrication technologies, which have been used for many years in the MEMS and microelectronics fields. Microfabrication technologies originate from the microelectronic industry, and the devices are usually made from silicon, even though glass, plastics, polymers, and many other materials are also in use. Silicon planar technology is currently the principle processing method in the fabrication of most silicon integrated circuits and devices, the history of which may be dated back to 1959 when Jean Hoerni and Robert Noyce developed this new process at Fairchild Semiconductor [95]. The microfabrication or micromachining for the designed microdevices generally contains the utilization of a set of manufacturing tools based on a batch of thin and thick film fabrication techniques commonly used in the electronics industry. In other aspects, it performs one of many engineering applications that makes use of serial direct micro/nano technologies, such as creating the modified and enhanced small three-dimensional (3D) structures with dimensions ranging from subcentimeters to submicrometers, including sensors, actuators, or microcomponents, microsystem, and much more traditional precision machining methods [97]. In our research project, the proposed novel micro-biosensor and chemical sensors were developed using the state of art microfabrication and nanofabrication facilities in the Institute for Micromanufacturing (IFM) at Louisiana Tech University, which fabricated some useful microfluidic devices [98-99].

4.3   Design of the Optical Detector

The proposed optical system for the fluorescence detection contains a light source which emits light at an appropriate wavelength ranging mainly around 466-470 nm, an objective lens, a collimator lens, a dichroic mirror, an excitation filter, an emission filter, and a photodetector built in the preamplifier in the optical path of the system. The excitation filter eliminates the unneeded light. The dichroic mirror is used for the light split of the excitation and the emission light path. The structure of the optical path in this system is shown in Figure 4.1. All the lenses and mirror devices are mounted mechanically to the housing and connected to each other to form a stable and miniaturized device.
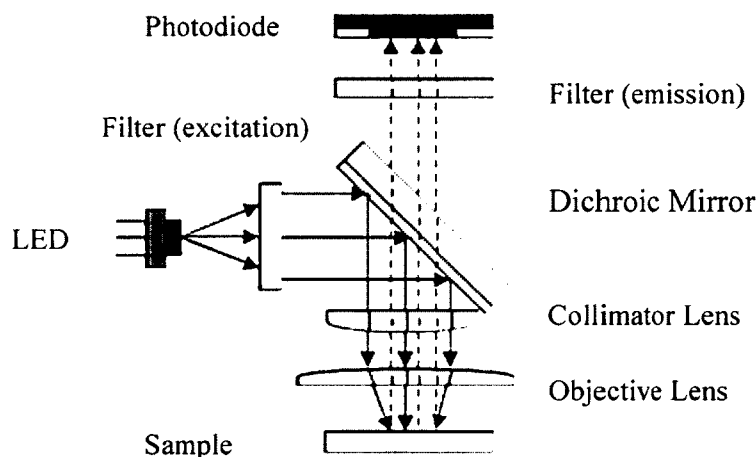
Figure 4.1 Structure of the optical path in the system.

The LED is applied as the light source in this system due to its advantages. In the past few years, the fluorescence detection system based on LED became very popular because of its low cost [100]. LED is much cheaper than other light sources, and it also has a long lifetime [29]. Here, we reviewed various advantages of using LED lighting in detail. Early stage of LEDs usually only achieve a low-intensity red light, but modern

products of it are available across the various visible range, such as ultraviolet and infrared wavelengths, with very high brightness and performance. LED can be integrated into our portable detection optical system as it is only a few milimeters in diameter as well as in length so that it may be easily installed. It is also easily obtained in the commercial market, with a low replacement costs every 10 or more years, and up to 100,000 hours lifetime, which is approximately 14 years, 18 hours per day usage. Moreover, it performs well and consumes 80% less energy than most traditional lighting products and is very durable with a very low maintenance record that is hard to break. So the small-sized LED products have become the prevalent replacement for many types of conventional lighting utilization. They are very economic and energy efficient with no wasted light or heat. There are many merits mentioned above, such as small size, long lifetime, fast switching, low energy consumption, robustness, and improved durability/reliability. They are also used as the replacements in many other different areas, such as in the traffic lights, aviation signals, and automotive lighting. The development of the sensors and the video displays relies on the possibility of compact size, fast switching, narrow bandwidth and great reliability of LEDs. Especially, the high switching rates allow the communications technology to be developed rapidly. There is another kind of LED which is infrared LED. It is most often utilized in the remote control units of commercial products, such as DVD players, televisions, and so on. It usually has a single-die shape used in many applications, such as indicators with different sizes from 2 mm to 8 mm. It also has two packages as through-hole and surface mount that are easy to design and no need for cooling the whole body. Also, the typical operation current

ranges from about 1 mA to above 20 mA. However, the type of LED needs a heat sink because it has a high current density [101].

4.4   <u>Structure of the Miniaturized Optical Fluorescence Detector</u>

The prototype of the system is shown in Figure 4.2, which is the picture of the fluorescence detector. The optical path in the system takes advantage of the dichroic mirror, excitation filter and different functional lenses to pass the light to the photodiode, which collects the emitted signals from the samples. The optical path starts with a blue LED light source. This system employs a water clear colored LED model ETG-5MN470-15, which has a peak emission wavelength of 470 nm with a luminous intensity of 3 cd (candela), and a viewing angle of 15°. Then the light passes through the excitation filter and is reflected from the dichroic mirror, which lets the light with 470 nm wavelength go through a collimator and an objective lens to focus on the sample. Then the fluorescence light about 518 nm wavelength from the sample is collimated by the same collimate lens, passes through the dichroic mirror, and then is detected by a photodiode after being filtered by an emitter filter. The photodiode collects the light signal and then immediately amplifies it with the amplification stage in the preamplifier, which is integrated in the photodiode-preamplifier.
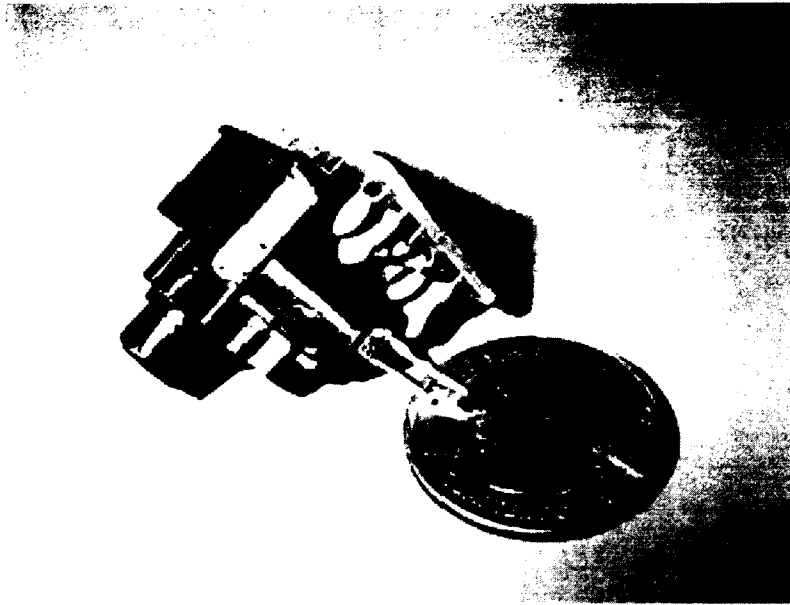
Figure 4.2 The picture of the fluorescence detection system.

The photodetector is an important component in the optical detection system. Diverse kinds of photodetectors contain photodiodes, avalanche photodiodes (APDs) [102-103], photomultiplier tubes (PMTs), and charge-coupled devices (CCDs). Currently, two common and versatile optical detectors are the photodiodes and the PMTs, which have complementary capabilities and are very widely used in optics. Both of them absorb light quanta (photons) and generate a current corresponding to the rate of photon absorption. Also, there are some other optical detection devices, including phototransistors, photoconductors, bolometers, pyroelectrics, and vidicons, etc. The bolometers and pyroelectrics function are based on the heat deposited by light absorbed in the detector. The vidicons are mainly for the original television camera tubes. They are all useful in the microfluidic detection area, which are also really very favorable for the silicon photocell used in solar power conversion. Among all of these photodetectors, the photodiode is operated to attain the optimum sensitivity and accuracy, suitable for the

system we discussed. However, all these detectors are expensive and very large, and incompatible with portable systems. Hence, in this project we have selected a blue/green enhanced 5 mm^2 silicon photodiode-preamplifier model ODA-6WB-500M, which features a large active area with extremely low noise and high sensitivity. The detector-preamplifier combination has a sensitivity of a wavelength response at 450 nm, typically 315 V/μW. It operates between 400 nm and 1100 nm with the peak frequency response at 940 nm and features 500 mega ohm transimpedance gain. It is easily integrated in an optical housing, and it is ideal for the fluorescence detection of low-light-level medical diagnostic applications because it has a few advantages over other systems. For example, the combined amplifier reduces both the outside and inside electrical and light signals' interference; thus, it enhances the ratio of signal and noise, as well as increasing the sensitivity of this system. Also, it is quite effective for the biomedical detection system. The emitter filter is mounted on it to filter the incident fluorescence light, then to generate the corresponding voltage to display on the multimeter which is processed by the low-noise amplifier and analog-digital converter inside the photodiode. However, it usually should be operated in complete darkness.

4.5   Experimental Results and Analysis

A set of experiments using a dilution series of fluorescence dye in DI water was conducted at the room temperature in order to investigate the capability of the designed fluorescence [82] detection system. A kind of fluorescence dye called 5-Carboxyfluorescein (5-FAM), which is an orange solid, was used in this testing experiment. 5-FAM is one of the most popular green fluorescent reagents used for biological and biomedical applications, such as in situ labeling peptides, proteins and

nucleotides. This chemical is used to provide various small fluorescent molecules. It has the spectral properties whose absorbance wavelength is 492 nm, and the emission wavelength is 518 nm. The solvent liquid that can be used here is Dimethylformamide (DMF) or DMSO. DMSO was applied in our experiment. It is a colorless liquid which is miscible in a variety of organic solvents, which is as useful as water. Also, this liquid dissolves both polar and nonpolar compounds inside for different applications.

The original sample solution was prepared by dissolving 0.5 mg 5-FAM into 1 mL DMSO liquid and then stirring them uniformly with sonication. Next, 70 μL of the original solution was diluted by adding DI water. Then each time portions of the previous sample were further diluted with DI water for the next testing. At last, the sample droplet was dripped onto the templet glass under the objective lens. The pipet was used to quantify the sample for the same dose every time. The dilution series started from a concentration of 86.92 μM down to 1.08 pM. The amplitude of the fluorescence signal was reflected by the measured voltage difference since the signal collected by the photodiode was converted to the electrical signal shown on the output. The plot of the fluorescein solution's concentrations versus the voltage differences within a long range interval of the concentration (10E-08 to 10E-12) is shown in Figure 4.3. It is found that the limit of detection of the fluorescein is 1.08 pM. In the meantime, the samples of the detailed different concentrations were also tested and then the curves were plotted in every different scale, such as shown in Figure 4.4 to Figure 4.8.

Delta Volts v.s. Concen. from 10E-08 to 10E-12 scale
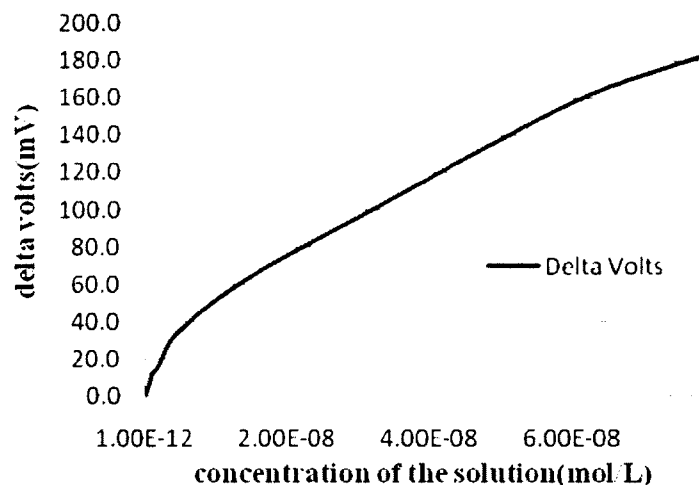
Figure 4.3 The relationship of the concentrations of the fluorescein solution samples range from 10E-08 to 10E-12 scale and the voltage differences.

Delta volts. v.s. Concen. in E-08
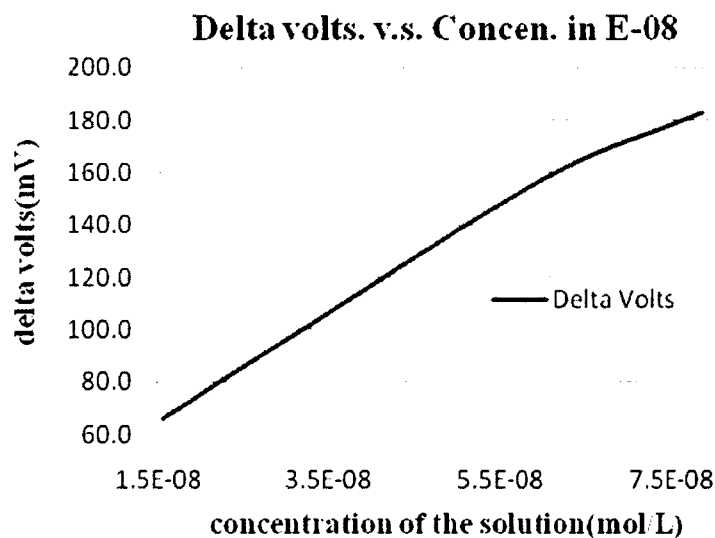
Figure 4.4 The relationship of the concentrations of the fluorescein solution samples and the voltage differences in 10E-08 scale.

Delta volts. v.s. Concen. in Nanoscale
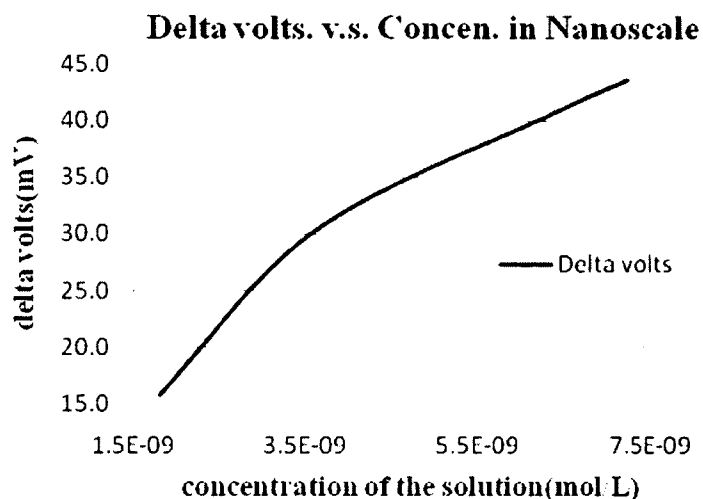
Figure 4.5 The relationship of the concentrations of the fluorescein solution samples and the voltage differences in nano-scale 10E-9.

Delta volts. v.s. Concen. in E-10
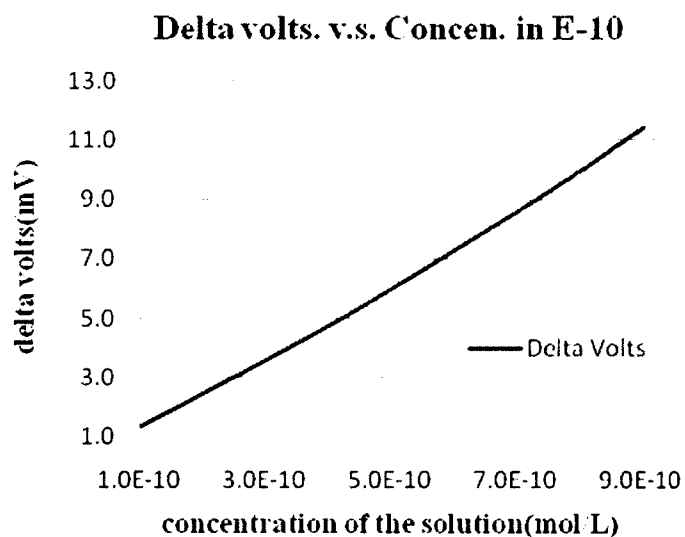
Figure 4.6 The relationship of the concentrations of the fluorescein solution samples and the voltage differences in 10E-10 scale.

Delta volts. v.s. Concen. in E-11
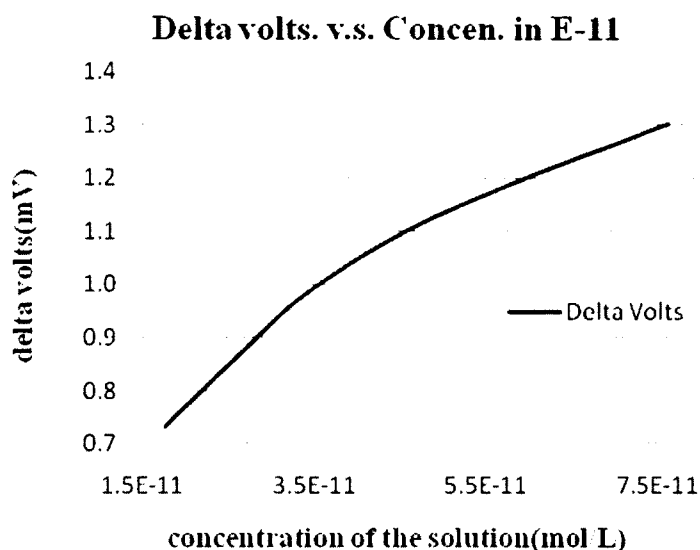
Figure 4.7 The relationship of the concentrations of the fluorescein solution samples and the voltage differences in 10E-11 scale.

Delta volts. v.s. Concen. in Pico-scale
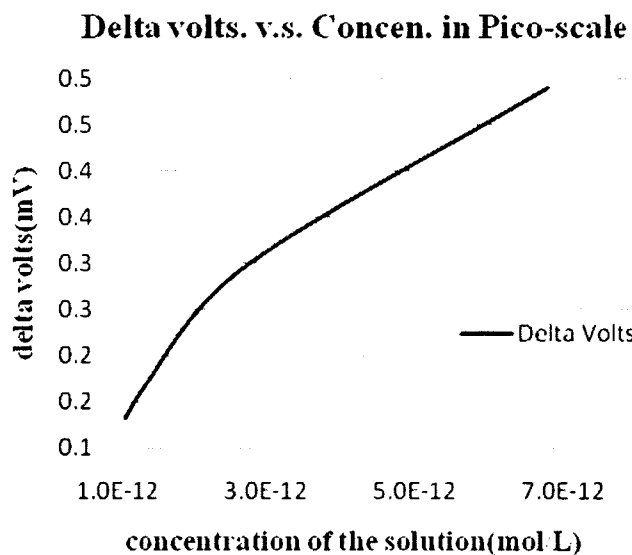
Figure 4.8 The relationship of the concentrations of the fluorescein solution samples and the voltage differences in pico-scale 10E-12.

From the plots we can know that the higher the concentration of the sample solution, the greater the voltage output will be, as we expected. When the concentration of the solution sample is increased, the corresponding voltage increases, too. A higher

concentration of the sample solution causes a higher output voltage, determining the intensity of the signal we collect. As we have tested, the sensitivity of the system is impressively at almost 1.08 pM. On some certain level, this is enough for the actual bioassay testing and detecting application. The sensitivity could also be increased by improving the housing of the system or the influence of the ambient light area. However, the operation of detection should be cautious, such as the adjustment of the focus lens, and so on. These factors all impact the testing and detecting results.

CHAPTER 5

CONCLUSIONS AND FUTURE WORK

5.1 Conclusions

A self-controlled and self-driven capillary system was developed here. A stop valve and a trigger valve on the microchip can manipulate the fluid flow in the capillary system without any external power supply or actuator. They are fabricated on a silicon wafer and sealed with a hydrophilic PEO-PDMS cover (the static water contact angle is 68°) to produce the autonomous microfluidic device. The static water contact angle of PEO-PDMS can reach stability from 21.5° to 80.9° when the PEO concentrations are at 1.9% to 0.2%. If the PEO concentration is increased over 2.0%, the contact angle can be further lowered; however, this PEO-PDMS film cannot be bonded on the wafer. In brief, the higher the concentration of the surfactant additive, the faster the fluid flows in the capillary channel. When the contact angle of the PEO-PDMS is about 80.9° or 58.5° (0.2% or 0.4% PEO concentration) and the expanding angle of the stop valve is 170°, the microfluidic chip works well with the water sample solution in the capillary action phenomenon. The PEO-PDMS with the adjustable contact angle can also be applied in other capillary phenomena with different viscous liquids. A high sensitivity, low cost and miniaturized optical detector was successfully developed and tested. To ensure high sensitivity, a superbright LED and a highly sensitive photodiode with the integrated

preamplifier are accepted as the light source and detection sensor. Meanwhile, these two parts and all necessary optical elements are integrated into one small package about 2 cm × 2 cm × 2 cm. The testing results prove a remarkable sensitivity at pico-scale molar size of about 1.08 pM. This cost-effective fluorescence detector can be easily integrated into any portable systems.

This research developed the cost-effective microfluidic capillary system and the miniaturized and highly sensitive optical detection system, which are the crucial parts of the POC testing apparatus. The research results prove that these two devices can be widely used for the LOC, the portable fluorescent detection devices or the systems for biological, chemical, medical and POC applications.

5.2 Future Work

There are still many challenges in the near future since the miniaturized bio-detection system normally deals with high sensitivity equipment, and the ratio of the signal to noise is crucial. Future work will focus on reducing background noises mixed with wanted detection signals to enhance the system sensitivity, because the electrical source of noise in our design will cause other peripheral problems close to electrical components. Consequently, a noise cancelling circuit can be designed and implemented in the future. It is also recommended that the silicon photomultiplier (SiPM) should replace the photodiode in the prototype. SiPM is a semiconductor device located on a common Si substrate, including many photon microcounters (10^3 mm^{-2}). SiPM operates in a limited Geiger mode and has a single photo electron gain (10^6) [104].

Another future work is to improve the capillary system on a chip in the fabrication process and the device designs. It is possible to make the surface of the capillary channels

hydrophilic and the stop valve's chamber hydrophobic. In this way, it will be easy to accurately control the fluid flow in the capillary channels. Meanwhile, the stop valve in the autonomous system will function better. However, the methods of the surface treatment are still under our consideration for further study.

Also, other functionalities can be added into the autonomous microfluidic system, such as safety features (flow resistances and delay valves) and timing features to enhance the system. Once the detection system, the microfluidic assay devices, and the microcontroller are all integrated, a complete biomedical diagnositic instrumentation will be established, which is a commonly used tool or a technique for the biological, clinical, and biomedical detection or data analysis systems.

REFERENCES

[1] Tüdős, A. J., Besselink, G. A. J., Schasfoortb, R. B. M., "Trends in Miniaturized Total Analysis Systems for Point-of-Care Testing in Clinical Chemistry," *Lab on a chip*, 1, 83-95, 2001.

[2] Gutcho, S., Mansbach, L., "Simultaneous Radioassay of Serum Vtamin B_{12} and Folic Acid," *Clinical Chemistry*, 23, 1609-1614, 1977.

[3] Vuori, J., Rasi, S., Takala, T., Vaananen, K., "Dual-label Time-Resolved Fluoroinmmunoassay for Simultaneous Detection of Myoglobin and Carbonic Anhydrase III in Serum," *Clinical Chemistry*, 37, 2087-2092, 1991.

[4] Xu, Y. Y., Pettersson, K., Blomberg, K., Hemmila, I., Mikola, H., Lovgren, T., "Simultaneous Quadruple-label Fluorometric Immunoaasay of Thyroid - Stimulating Hormone, 17 Alpha-Hydroxyprogesterone, Immunoreactive Trypsin, and Creatine Kinase MM Isoenzyme in Dried Blood Spots," *Clinical Chemistry*, 38, 2038-2043, 1992.

[5] Brown, C. R., Higgins, K. W., Frazer, K., Schoelz, L. K., Dyminski, J. W., Marinkovich, V. A., Miller, S. P., Burd, J. F., "Simultaneous Determination of Total IgE and Allergen-Specific IgE in Serum by the MAST Chemiluminescent assay system," *Clinical Chemistry*, 31, 1500-1505, 1985.

[6] Hayes, F. J., Halsall, H. B., Heineman, W. R., "Simultaneous Inmmnoassay Using Electrochemical Detection of Metal Ion Labels," *Analytical Chemistry*, 66, 1860-1865, 1994.

[7] Butler, J. E., "Characerization of the Soluble Immune Complex (EIC) of the Amplified Enzyme-Linked Immunosorbent Assay (a-ELISA) and an Evaluation of this Assay for Quantitation by Reaction Stoichiometry," *Journal of Immunoassay*, 21, 165-209, 2000.

[8] Wegner, G. J., Lee, H. J., Corn, R. M., "Characteization and Optimization of Peptide Arrays for the Study of Epitope-Antibody Interactions Using Surface Plasmon Resonance Imaging," *Analytical Chemistry*, 74, 5161-5168, 2002.

[9] Rohr, T. E., Cotton, T., Fan, N., Tarcha, P. J., "Immunoassay Employing Surface-Enhanced Raman Spectroscopy," *Analytical Biochemistry*, 182, 388-398, 1989.

[10] Mattoussi, H., Mauro, J. M., Goldman, E. R., Anderson, G. P., Sundar, V. C., Mikulec, F. V., Bawendi, M. G. J., "Self-Assembly of CdSe-ZnS Quantum Dot Bioconjugates Using an Engineered Recombinant Protein," *Journal of American Chemical Society*, 122, 12142-12150, 2000.

[11] Wu, G., Datar, R. H., Hansen, K. M., Thundat, T., Cote, R. J., Majumdar, A., "Bioassay of Prostate-Specific Antigen (PSA) Using Microcantilevers," *Nature Biotechnology*, 19, 856-860, 2001.

[12] Grogan, C., Raiteri, R., O'Connor, G. M., Glynn, T. J., Cunningham, V., Kane, M., Charlton, M., Leech, D., "Characterization of an Antibody Coated Microcantilever as a Potential Immune-Based Biosensor," *Biosensors Bioelectronics*, 17, 201-207, 2002.

[13] Baselt, D. R., Lee, G. U., Colton, R. J., "Biosensor Based on Force Microscope Technology," *Journal of Vacuum Science and Technology B*, 14 (2), 789-796, 1996.

[14] Grubisha, D. S., Liper, R. J., Park, H, Y., Driskell, J., Porter, M. D., "Femtolar Detection of Prostate-Specific Antigen: An Immunoassay Based on Surface-Enhanced Raman Scattering and Immunogold Labels," *Analytical Chemistry*, 75 (21), 5936–5943, 2003.

[15] Joseph Wang, "Electrochemical Biosensors: Towards Point-of-Care Cancer Diagnostics," *Biosensors and Bioelectronics*, 21(10), 1887-1892, 2006.

[16] Yang, T. J., Lessard, Guillaume A., Quake, S. R., "An Apertureless Near-Field Microscope for Fluorescence Imaging," *Applied Physics Letters*, 76(3), 378 – 380, 2000.

[17] Dunn, K.W. Mayor, S., Myers, J. N., Maxfield, F. R., "Applications of Ratio Fluorescence Microscopy in the Study of Cell Physiology," *The Journal of the Federation of American Societies for Experimental Biology*, 8, 573-582, 1994.

[18] Lee, S. J., Lee, S. Y., "Micro Total Analysis System (micro-TAS) in Biotechnology," *Applied Microbiology and Biotechnology*, 64 (3), 289-299, 2004.

[19] Ichikawa, N., Hosokawa, K., Maeda, R., "Interface Motion of Capillary-Driven Flow in Rectangular Microchannel," *Journal of Colloid and Interface Science*, 280 (1), 155-164, 2004.

[20] Stange, M., Dreyer, M. E., Hans J. Rath, H. J., "Capillary Driven Flow in Circular Cylindrical Tube," *Physics of Fluids*, 15 (9), 2587-2601, 2003.

[21] Reyes, D. R., Iossifidis, D., Auroux, P. A., Manz, A., "Micro Total Analysis Systems: Introduction, Theory, and Technology," *Analytical Chemistry*, 74, 2623-2636, 2002.

[22] Dittrich, B., Hübschle, C. B., Luger, P., Spackman, M. A., "Introduction and Validation of an Invariom Database for Amino-Acid, Peptide and Protein Molecules," *Acta Crystallographica Section D: Biological Crystallography*, 62 (11), 1325-1335, 2006.

[23] Dittrich P. S., Tachikawa, K., Manz, A., "Micro Total Analysis Systems. Latest Advancements and Trends," *Analytical Chemistry*, 78, 3887-3907, 2006.

[24] Bally, M., Halter, M., Voros J., Grandin, H. M., "Optical Microarray Biosensing Techniques," *Surface and Interface Analysis*, 38, 1442-1458, 2006.

[25] Sia, S. K., Linder, V., Parviz, B. A., Siegel, A., Whitesides, G. M., "An Integrated Approach to a Portable and Low-Cost Immunoassay for Resource-Poor Settings," *Angewandte Chemie International Edition*, 43 (4), 498-502, 2004.

[26] Linder, V., Sia, S. K., Whitesides, G. M., "Reagent-Loaded Cartridges for Valveless and Automated Fluid Delivery in Microfluidic Devices," *Analytical Chemistry*, 77, 64-71, 2005.

[27] Balslev, S., Jorgensen, A. M., Bilenberg, B., Mogensen, K. B., Snakenborg, D., Geschke, O., Kutter, J. P., Kristensen, A., "Lab-on-a-Chip with Integrated Optical Transducers," *Lab on a Chip*, 6, 213-217, 2006.

[28] Jung, M. Y., Choi, S. S., "Fabrication of Bimetallic Cantilevers and its Characterization," *Surface Review and Letters*, 6 (6), 1195-1199, 1999.

[29] Tang, Y., Fang, J., Yan, X., Ji, H. F., "Fabricaiton and Characterization of SiO2 Microcantilever for Microsensor Application," *Sensors and Actuators B*, 97, 109-113, 2004.

[30] Yan, X., Tang, Y., Ji, H. F., "Nerve Agent Biosensing Using an Enzyme Coated Microcantilever," *Instrumentation Science & Technology*, 32 (2), 175-183, 2004.

[31] Tang, Y., Fang, J., Ji, H. F., Brown, G. M., Thundat, T., "Detection of Femtomolar Concentration of HF Using a SiO_2 Microcantilever," *Analytical Chemistry*, 76, 2478-2481, 2004.

[32] Zeng, J., Deshpande, M., Greiner, K. B., Gilbert, J. R., "Fluidic Capacitance Model of Capillary-Driven Stop Valves," in: *Proceedings of ASME International Mechanical Engineering Congress and Exposition*, 2000, 1-7.

[33] Tan, S. H., Nguyen, N. T., Chua, Y. C., Kang, T. G, "Oxygen Plasma Treatment for Reducing Hydrophobicity of a Sealed Polydimethylsiloxane Microchannel," *Biomicrofluidics*, 4, 032204-1-032204-8, 2010.

[34] Gliere, A., Delattre, C., "Modeling and Fabrication of Capillary Stop Valves for Planar Microfluidic Systems," *Sensors and Actuators A: Physical*, 130-131, 601-608, 2006.

[35] Man, P. F., Mastrangelo, C. H., Burns, M. A., Burke, D. T., "Microfabricated Capillary Driven Stop Valves and Sample Injector," In: *Proceedings of the 11th Annual International Workshop on MEMS conference*, 1998, 25-29.

[36] Cho, H., Kim, H. Y., Kang, J. Y., Kim, T. S., "How the Capillary Burst Microvalve Works," *Journal of Colloid Interface Science*, 306 (2), 379-385, 2007.

[37] Cha, J. H., Kim, J., Ryu, S. K., Park, J. Y., Jeong, Y. W., Park, S., Park, S. K., Kim, H. C., Chun, K., "A Highly Efficient 3D Micromixer Using soft PDMS Bonding" *Journal of Micromechanics and Microengineering*, 16, 1778-1782, 2006.

[38] Mitchell, P., "Microfluidics-Downsizing Large-Scale Biology," *Nature Biotechnology*, 19 (8), 717-721, 2001.

[39] Kopp, M. U., Crabtree, H. J., Manz, A., "Developments in Technology and Applications of Microsystems," *Chemistry & Biology*, 1 (3), 410-419, 1997.

[40] Colyer, C .L., Tang, T., Chiem, N., Harrison, D. J., "Clinical Potential of Microchip Capillary Electrophoresis Systems," *Electrophoresis*, 18 (10), 1733-1741, 1997.

[41] Schult, K., Katerkamp, A., Trau, D., Grawe, F., Camman, K., Meusel, M., "Disposable Optical Sensor Chip for Medical Diagnostics: New Ways in Bioanalysis," *Analytical Chemistry*, 71 (23), 5430-5435, 1999.

[42] Wang, J., Rivas, G., Cai, X., Palecek, E., Nielsen, P., Shiraishi, H., Dontha, N., Luo, D., Parrado, C., Chicharro, M., Farias, P., Valera, F. S., Grant, D. H., Ozsoz, M., Flair, M. N., "DNA Electrochemical Biosensors for Environmental Monitoring. A Review," *Analytica Chimica Acta*, 347 (1-2), 1-8, 1997.

[43] Reyes, D. R., Iossifidis, D., Auroux, P. A., Manz, A., "Electrodeless Dielectrophoresis for Micro Total Analysis Systems," *IEEE Engineering in Medicine and Biology*, 3, 62-67, 2003.

[44] Van de Schoot, B. H., Verpoorte, E. M. J., Jeanneret, S., Manz, A., Rooij, N. R., "Microsystems for Analysis in Flowing Solutions," In: *Proceedings of the Micro Total Analysis Systems*, 1994, 181-190.

[45] Northrup, M. A., Benett, B., Hadley, D., Stratton, P., Landre, P., "Advantages Afforded by Miniaturization and Integration of DNA Analysis Instrumentation," In: *Proceedings of the 1st International Conference on Microreaction Technology*, 1997, 278-288.

[46] Ramsey J. M., Widmer, E., Verpoorte, E., Eds, "Miniature Chemical Measurement Systems," In: *Proceedings of the 2nd International Symposium on Miniaturized Total Analysis Systems*, 1996, 24-29.

[47] Blankenstein, G., Larsen, U. D., "Modular Concept of a Laboratory on a Chip for Chemical and Biochemical Analysis," *Biosensors and Bioelectronics*, 13 (3-4), 427-438, 1998.

[48] Nilsson, S., Laurell, T., "Miniaturization in Analytical and Bioanalytical Chemistry," *Analytical and Bioanalytical Chemistry*, 378 (7), 1676-1677, 2004.

[49] Nguyen, N. T., Wereley, S. T., *Fundamentals and Applications of Microfluidics*. Boston: Artech House, 2002.

[50] Selvaganathy, P., Carlen, E. T., Mastranglo, C. H., "Electrothermally Actuated Inline Microfluidic Valve," *Sensors and Actuators A: Physical*, 104 (3), 275-282, 2003.

[51] Esashi, M., Shoji, S., Nakano, A., "Normally Closed Microvalve and Micropump Fabricated on a Silicon Wafer," *Sensors and Actuators A*, 20 (1-2), 163-169, 1989.

[52] Andersson, H., Wijngaart, W., Griss, P., Niklaus, F., Stemme, G., "Hydrophobic Valves of Plasma Deposited Octafluorocyclobutane in DRIE Channels," *Sensors and Actuators B: Chemical*, 75, 136-141, 2001.

[53] Zoval, J. V., Madou, M. J., "Centrifuge Based Fluidic Platforms," In: *Proceedings of IEEE*, 2004, 92 (1), 140-153.

[54] Lauks, I. R., Wieck, H. J., Zelin, M. P., Blyskal, P., "Disposable Sensing Device for Real Time Fluid Analysis." US patent N° 5, 096, 669, 1994.

[55] Kugelmass, S. M., Lin, C., DeWitt, S. H., "Fabrication and Characterization of Three-Dimensional Microfluidic Arrays," In: *Proceedings of SPIE 3877 on Microfluidics Devices and Systems II*, 1999, 88.

[56] McNeely, M. R., Spute, M. K., Tusneem, N. A., Oliphant, A. R., "Hydrophobic Microfluidics," In: *Proceedings of SPIE 3877 on Microfluidic Devices and Systems II*, 1999, 210.

[57] Handique, K., Burke, D. T., Mastrangelo, C. H., Burns, M. A., "Nanoliter Liquid Metering in Microchannels Using Hydrophobic Patterns," *Analytical Chemistry*, 72 (17), 4100-4109, 2000.

[58] Melin, J., Roxhed, N., Gimenez, G., Griss, P., van der Wijngaart, W., Stemme, G., "A Liquid-Triggered Liquid Microvalve for On-Chip Flow Control," *Sensors and Actuators B: Chemical*, 100 (3), 463-468, 2004.

[59] Anderson, J. M., Ziats, N. P., Azeez, A., Brunstedt, M. R., Stack, S., Bonfield, T. L., "Protein Adsorption and Macrophage Activation on Polydimethylsiloxane and Silicone Rubber," *Journal of Biomaterials Science, Polymer Edition*, 7 (2), 159-169, 1996.

[60] Yamamoto, T., Fujii, T., Nojima, T., "PDMS-Glass Hybrid Microreactor Array with Embedded Temperature Control Device. Application to Cell-Free Protein Synthesis," *Lab Chip*, 2, 197-202, 2002.

[61] Cha, J. H., Kim, J., Ryu, S. K., Park, J. Y., Jeong, Y. W., Park, S., Park, S. K., Kim, H. C., Chun, K., "A Highly Efficient 3D Micromixer Using soft PDMS Bonding" *Journal of Micromechanics and Microengineering*, 16, 1778-1782, 2006

[62] Hong, S., Kim, S., Kim, J., Hwang, H., "Hydrophilic surface modification of PDMS using atmospheric RF plasma," *Journal of Physics*, 34, 656-661, 2006.

[63] Fritz, J. L., Owen, M. J., "Hydrophobic Recovery of Plasma-Treated Polydimethylsiloxane," *Journal of Adhesion Science and Technology*, 54, 33-45, 1995.

[64] Hocker, H., "Plasma Treatment of Textile Fibers." *Pure and Applied Chemistry*, 74 (3), 423-427, 2002.

[65] Makamba, H., Kim, J. H., Lim, Park, K. N., Hahn, J. H., "Surface Modification of Poly(dimethylsiloxane) Microchannels," *Electrophoresis*, 24, 3607, 2003.

[66] Wong, I., Ho, C. M., "Surface Molecular Property Modifications for Poly (dimethylsiloxane) (PDMS) Based Microfluidic Devices," *Microfluidics and Nanofluidics*, 7 (3), 291-306, 2009.

[67] Zhou, J. Ellis, A. V., Voelcker, N. H., "Recent Developments in PDMS Surface Modification for Microfluidic Devices," *Electrophoresis*, 31, 2-16, 2010.

[68] Kasemura, T., Takahashi, S., Okada, T., Maegawa, T., Oshibe, T., "Surface Dynamics for Poly(vinyl alkylate)s via Dynamic Contact Angle and Adhesion Tension Relaxation," *Elsevier Science: Polymer*, 37 (16), 3659-3664, 1996.

[69] Yang, J., Wenger, G., Koningsveld, R., "Phase Behavior of Ethylene Oxide-Dimethylsiloxane PEO-PDMS-PEO Triblock Copolymers with Water," *Colloid & Polymer Science*, 270 (11), 1080-1084, 1992.

[70] Decher, G., "Fuzzy Nanoassemblies: Toward Layered Polymeric Multicomposites," *Science*, 227, 1232-1237, 1997.

[71] Lvov, Y., Decher, G., "Assembly, Structural Characterization and Thermal Behavior of Layer-by-Layer Deposited Ultrathin Films of Polyvinylsulfate and Polyallylamine," *Langmuir*, 9, 481-486, 1993.

[72] Keller, S., Kim, H. N., Mallouk, T., "Layer-by-Layer Assembly of Intercalation Compounds and Superlattices on Surfaces: Towards Molecular 'Beaker' Epitaxy," *Journal of American Chemical Society*, 116, 8817-8821, 1994.

[73] Ai, H., Lvov, M. Y., Mills, D. K., Meng, H., Qiao, Xi., "Coating Bio-Nanofilm on PDMS Through Layer-by-Layer Self-Assembly," *Engineering in Medicine and Biology*, 1, 608-609, 2002.

[74] Yu, K., Han, Y. C., "A Stable PEO-Tethered PDMS Surface Having Controllable Wetting Property by a Swelling-Deswelling Process," *Soft Matter*, 2, 705-709, 2006.

[75] McDonald J. C., Duffy, D. C., Anderson, J. R., "Fabrication of Microfluidic Systems in Poly(dimethylsiloxane)," *Electrophoresis*, 21, 27-40, 2002.

[76] Thorsen, T., Maerkl, S. J., Quake, S. R., "Microfluidic Large-Scale Integration," *Science*, 298, 580-584, 2002.

[77] Laermer, F., Schilp A., "Method of Anisotropically Etching Silicon." U. S. Patent 5501893, 1996.

[78] Laermer, F., Schilp, A., Funk, K., Offenberg, M., "Bosch Deep Silicon Etching: Improving Uniformity and Etch Rate for Advanced MEMS Applications," In: *Proceedings Tech. Dig. MEMS*, 1999, 211-216.

[79] Quevy, E., Parvais, B., Raskin, J. P., Buchaillot, L., Flander, D., Collard, D., "A Modified Bosch-Type Process for Precise Surface Micromachining Polysilicon," *Journal of Micromechanics and Microengineering*, 12, 328-333, 2002.

[80] Cha, J. H., Kim, J., Ryu, S. K., Park, J. Y., Jeong, Y., Park, S., Park, S. H., Kim, S. C., Chun, K. J., "A Highly Efficient 3D Micromixer Using Soft PDMS Bonding," *Journal of Micromechanics and Microengineering*, 16, 1778-1782, 2006.

[81] Egidi, G., Herrera, F., Moreno-Bondi, M. C., Kempe, M., Van Rhijn, J. A., Fiaccabrino, G. C., de Rooij, N. F., "Fabrication and Characterization of Stop Flow Valves for Fluid Handling," In: *Proceedings of the 12th International Conference on Solid-State Sensors, Actuators and Microsystems*, 2003, 147-150.

[82] Dhruv, H. D., "Controlling Nonspecific Adsorption of Proteins at Bio-Interfaces for Biosensor and Biomedical Applications." Ph.D Dissertation, Utah State University, USA, 2009.

[83] Wang, W., Zhou, L., Wang, S., Luo, Z., Hu, Z., "Rapid and Simple Determination of Adenine and Guanine in DNA Extract by Micellar Electrokinetic Chromatography with Indirect Laser-Induced Fluorescence Detection," *Talanta*, 74 (4), 1050, 2008.

[84] Du, X. L., Zhang, H. S., Deng, Y. H., Wang, H., "Design and Synthesis of a Novel Fluorescent Reagent, 6-Oxy-(Ethylpiperazine)-9-(2-Methoxycarbonyl) Fluorescein, for Carboxylic Acids and its Application in Food Samples Using High-Performance Liquid Chromatography," *Journal of Chromatography A*, 1178, 92, 2008.

[85] Nakamura, M., Tsumoto, K., Ishimura, K., Kumagai, I., "Detection of Biotinylated Proteins in Polyacrylamide Gels Using an Avidin-Fluorescein Conjugate," *Analytical Biochemistry*, 304 (2), 231-235, 2002.

[86] Guilbault, G. G., *Practical Fluorescence*, second edition, CRC Press, 1990.

[87] Popp, J., Strehle, M., *Biophotonics: Visions for Better Health Care*, Wiley-VCH, 2006.

[88] Srinivasan, V., Pamula, V. K., Fair, R. B., "An Integrated Digital Microfluidic Lab-on-Chip for Clinical Diagnostics on Human Physiological Fluids," *Lab on a Chip*, 310-315, 2004.

[89] Kostner, S., Vellekoop, M. J., "Detection of Single Biological Cells Using a DVD Pickup Head," In: *Proceedings of International IEEE Solid-State Sensors, Actuators and Microsystems Conference*, 2007, 2123-2126.

[90] Chediak, J. A., Luoa, Z., Seo, J., Cheungc, N., Lee L. P., Sandse, T. D., "Heterogeneous Integration of Cds Filters with GaN LEDs for Fluorescence Detection Microsystems," *Sensors and Actuators A*, 111 (1), 1-7, 2004.

[91] Seo, J., Lee, L. P., "Disposable Integrated Microfluidics with Self-Aligned Planar Microlenses," *Sensors and Actuators B*, 99, 615-622, 2004.

[92] Yang, H., Lee, C. T., "Miniaturized Fluorescence Excitation Platform with Optical Fiber for Bio-Detection Chips," in *DTIP*, TIMA Editions, 2006, 1-5.

[93] Optical detection:
http://www.flowinjection.com/fluorometersandspectrometers.html.

[94] Klotzkin, D., Papautsky, I., "High-Sensitivity Integrated Fluorescence Analysis for Microfluidic Lab-on-a-Chip," In: *Proceedings of SPIE Newsroom*, 2007, 1-3.

[95] Hung, K. Y., Tseng, F. G., Khoo, H. S., "Integrated Three-Dimensional Optical MEMS for Chip-Based Fuorescence Detection," *Journal of Micromechanics and Microengineering*, 19 (4), 1-10, 2009.

[96] Kostal, V., Zeisbergerova, M., Slais, K., Kahle, V., "Fluorescence Detection System for Capillary Separations Utilizing a Liquid Core Waveguide with an Optical Fibre-Coupled Compact Spectrometer," *Journal of Chromatography A*, 1081 (1), 36-41, 2005.

[97] Novak, L., Neuzil, P., Pipper, J., Zhang, Y. and Lee, S., "An Integrated Fluorescence Detection System for Lab-on-a-Chip Applications," *Lab Chip*, 7, 27-29, 2007.

[98] Shen, B., Xie, Y., Irawan, R., "A Novel Portable Fluorescence Detection System for Microfluidic Card," *Journal of Instrumentation*, 3, 1-11, 2008.

[99] Chin, C. D., Linder, V., Sia, S. K., "Lab-on-a-Chip Devices for Global Health: Past Studies and Future Opportunities," *Lab Chip*, 7, 41-57, 2007.

[100] Dasgupta, P. K., Eom, I. Y., Morris, K. J., Li, J. Z., "Light Emitting diode-based Detectors-Absorbance, Fluorescence and Spectroelectrochemical Measurement in a Planar Flow-Through Cell," *Analytica Chimica Acta*, 500 (1-2), 337-364, 2003.

[101] Braunstein, R., "Radiative Transitions in Semiconductors," *Journal of Physics*, 99 (6), 1892-1893, 1955.

[102] Dereniak, E. L., Crowe, D. G., *Optical Radiation Detectors*. NewYork: Wiley, 1984, 57-68.

[103] Wegrzecki, M., Grynglas, M., Bar, J., Uszynski, A., Grodecki, R., Grabiec, P., Krzeminski, S., Budzynski, T., "Design and Properties of Silicon Avalanche Photodiodes," *Opto-Electronics Review Journal*, 12 (1), 95-104, 2004.

[104] Buzhana, P., Dolgoshein, B., Filatov, L., Ilyina, A., Kantzerov, V., Kaplin, V., Karakash, A., Kayumovc, F., Klemin, S., Popova, E., Smirnov, S., "Silicon Photomultiplier and Its Possible Applications," *Nuclear Instruments and Methods in Physics Research A*, 504, 48-52, 2003.